U.S. DEPARTMENT OF COMMERCE
NATIONAL OCEANIC AND ATMOSPHERIC ADMINISTRATION
NATIONAL WEATHER SERVICE
NATIONAL METEOROLOGICAL CENTER

OFFICE NOTE 200[1]

Multivariate Analysis of Temperatures and Winds Using Optimum Interpolation

Kenneth H. Bergman
Development Division

MAY 1979

---

[1] Also submitted for publication in Monthly Weather Review.

ABSTRACT

The design of a statistical "optimum interpolation" analysis system for multivariate analysis of temperature and wind fields is described. The scheme uses three-dimensional correlation functions, defined as products of quasi-horizontal and vertical correlations. A numerical prediction is used to provide background fields, and corrections to them are obtained using optimum interpolation. Observations are assigned rms error levels, and for some observational types the errors are assumed to be vertically or laterally correlated. A procedure for using oceanic surface data in the upper-air analysis is included.

Some special design features, including data selection and error-checking procedures, are discussed. The mechanics of the analysis system are illustrated with a step-by-step example analysis. Several experimental analyses are compared in order to illustrate sensitivity of the analysis scheme to changes in design features and governing parameters.

1. Introduction

In an era when the meteorological observing network is composed of a number of different observing systems, each with its own quality characteristics, it is desirable to use a method of data analysis which accounts for these differences in a logical and systematic manner. An analysis method which accomplishes this goal and has other desirable properties is that of optimum interpolation.

First developed comprehensively by L. S. Gandin (1963), optimum interpolation is an analysis scheme which estimates the value of a meteorological field at any desired set of locations from a "guess" value at each location and the observations in the vicinity of each location. Normally, the set of locations comprises a regular grid network, and the guess values are provided by a forecast, climatology, or a blend of the two. When a forecast is used to provide the guess field, the optimum interpolation analysis is said to "update" the forecast field in those regions where current synoptic data are available.

The analysis scheme presented here is designed to update values of temperature and horizontal wind components at the grid points of a nine-layer global prediction model (Stackpole et al., 1974) currently in operational use at the National Meteorological Center (NMC). It is multivariate; wind observations are used in the interpolative analysis

of the temperature field and vice versa. Geostrophy, in the form of the thermal wind relationship (as suggested by Eddy, 1973), is used to determine the impact of one type of data on the other type of field. Thus, a degree of mass-momentum balancing is provided by the analysis that would not be present if the temperature and wind fields were analyzed separately.

The theoretical basis for the multivariate analysis of meteorological fields by optimum interpolation is outlined by Gandin (1963), and Gandin and Kagan (1974). Multivariate analysis of geopotential height was performed for a single grid point by Kluge (1970), who concluded that the inclusion of wind information improved the accuracy of the height analysis. Working versions of multivariate analysis of heights and winds on isobaric surfaces have been developed by Rutherford (1973, 1976), Schlatter (1975), and Schlatter et al. (1976). Many of the design features of these two optimum interpolation schemes have been incorporated in the present system. An earlier version of the analysis system is summarized by Bergman (1976).

2. Formulation of analysis equations

Consider a regular grid of points in three dimensions (λ, ϕ, p) where current values of meteorological fields are desired. Assume that "guess" values of the fields are known at each grid point. These guess values might be provided by a numerical forecast (Kruger, 1969), by climatological normals (Gandin, 1963), or by a suitable blend of the two.

Assume that there is an irregular distribution of observations of the meteorological variables, for example temperature and the two wind components, for which values are desired at the grid points. These observations may be taken by a heterogeneous collection of observing systems, such as rawinsonde, satellite, aircraft, etc. The horizontal location and pressure-altitude of each observation are assumed known.

Using bilinear interpolation in latitude-longitude and linear in $\ell n(p)$ in the vertical, the values of the guess fields at each observation location may be determined, and the difference between each observed value and corresponding guess value may be computed; thus,

$$\hat{f}_{ik} = \hat{F}_{ik} - \tilde{F}_{ik} \ , \tag{2.1}$$

where $\hat{f}_{ik}$ is this difference (or residual) for the i^{th} observation of the k^{th} variable, $\hat{F}_{ik}$ is the observed value, and $\tilde{F}_{ik}$ is the corresponding guess value of the k^{th} variable at the same location. When more than one variable is measured by an instrument at a particular location, each measurement counts as a separate observation.

Each observation is to some extent erroneous. Thus,

$$\hat{F}_{ik} = F_{ik} + e_{ik}, \tag{2.2}$$

where F_{ik} is the "true" value of the k^{th} variable at the location of the i^{th} observation and e_{ik} is the observational error. Similarly,

$$\hat{f}_{ik} = f_{ik} + e_{ik} \ ,$$

where

$$f_{ik} \equiv F_{ik} - \tilde{F}_{ik} \tag{2.4}$$

is the difference between the true value of the k^{th} variable and the first guess at the i^{th} location.

The true value F_{gr} of the r^{th} variable at a representative grid point may be estimated by

$$F_{gr} \simeq \tilde{F}_{gr} + \sum_{k=1}^{m} \sum_{i=1}^{n_k} a_{ik} \hat{f}_{ik}, \tag{2.5}$$

where $\tilde{F}_{gr}$ is the guess value of F_{gr} at the grid point, m is the number of variables entering into the multivariate analysis of variable r at grid point g, n_k is the number of observations of variable k used in the analysis, and a_{ik} is the weight which the i^{th} observation of type k receives in forming the estimate of F_{gr}.

In general, the right-hand side of (2.5) will not give the true value F_{gr} of variable r at the grid point but will differ by an amount called the analysis error. Statistical optimum interpolation requires that the mean square analysis error E_{gr}^2 of (2.5),

$$E_{gr}^2 = \overline{[F_{gr} - \tilde{F}_{gr} - \sum_{k=1}^{m} \sum_{i=1}^{n_k} a_{ik}(f_{ik} + e_{ik})]^2}, \tag{2.6}$$

be a minimum, where the bar denotes an ensemble average over a large number of grid point analysis situations. This requirement results in the following set of equations:

$$\sum_{\ell=1}^{m} \sum_{j=1}^{n_\ell} (\overline{f_{ik} f_{j\ell}} + \overline{f_{ik} e_{j\ell}} + \overline{e_{ik} f_{j\ell}} + \overline{e_{ik} e_{j\ell}}) a_{j\ell} = \overline{f_{ik} f_{gr}} + \overline{e_{ik} f_{gr}}, \tag{2.7}$$

$$k = 1,2,\ldots,m; \; i = 1,2,\ldots,n_k.$$

If the weights $a_{j\ell}$ satisfy these equations, then E_{gr}^2 can be re-expressed in the form (Gandin and Kagan, 1974)

$$E_{gr}^2 = \overline{f_{gr}^2} - \sum_{k=1}^{m} \sum_{i=1}^{n_k} a_{ik}(\overline{f_{ik} f_{gr}} + \overline{e_{ik} f_{gr}}). \tag{2.8}$$

In (2.7) and (2.8), f_{gr} is the difference between F_{gr} and $\tilde{F}_{gr}$; see (2.4).

The set of equations (2.7) can be solved for the observational weights a_{ik} provided the statistical covariances $\overline{f_{ik}f_{j\ell}}$, $\overline{f_{ik}e_{j\ell}}$, etc., are known or can be estimated. Then the statistically optimum value of F_{gr} is given by (2.5) using these weights, and the corresponding estimate of analysis error for F_{gr} is provided by (2.8).

It is convenient to re-express equations (2.7) and (2.8) in normalized form. Dividing each equation of (2.7) by $\left(\overline{f_{ik}^2}\,\overline{f_{gr}^2}\right)^{\frac{1}{2}}$ yields

$$\sum_{\ell=1}^{m}\sum_{j=1}^{n_\ell}\left(\rho_{ij}^{k\ell}+\tau_{ij}^{k\ell}\epsilon_{j\ell}+\tau_{ji}^{\ell k}\epsilon_{ik}+\eta_{ij}^{k\ell}\epsilon_{ik}\epsilon_{j\ell}\right)a'_{j\ell}=\rho_{ig}^{kr}+\tau_{gi}^{rk}\epsilon_{ik}, \qquad (2.9)$$

$$k = 1,2,\ldots,m;\ i = 1,2,\ldots,n_k;$$

where

$$\rho_{ij}^{k\ell} \equiv \left(\overline{f_{ik}f_{j\ell}}\right)\Big/\left(\overline{f_{ik}^2}\,\overline{f_{j\ell}^2}\right)^{\frac{1}{2}}, \qquad (2.10a)$$

$$\tau_{ij}^{k\ell} \equiv \left(\overline{f_{ik}e_{j\ell}}\right)\Big/\left(\overline{f_{ik}^2}\,\overline{e_{j\ell}^2}\right)^{\frac{1}{2}} \qquad (2.10b)$$

$$\eta_{ij}^{k\ell} \equiv \left(\overline{e_{ik}e_{j\ell}}\right)\Big/\left(\overline{e_{ik}^2}\,\overline{e_{j\ell}^2}\right)^{\frac{1}{2}} \qquad (2.10c)$$

$$\epsilon_{ik} \equiv \left(\overline{e_{ik}^2}/\overline{f_{ik}^2}\right)^{\frac{1}{2}}, \qquad (2.10d)$$

and

$$a'_{j\ell} \equiv \left(\overline{f_{j\ell}^2}/\overline{f_{gr}^2}\right)^{\frac{1}{2}}a_{j\ell}. \qquad (2.10e)$$

Division of (2.8) by $\overline{f_{gr}^2}$ gives

$$E_{gr}^2\Big/\left(\overline{f_{gr}^2}\right) = 1 - \sum_{k=1}^{m}\sum_{i=1}^{n_k}a'_{ik}\left(\rho_{ig}^{kr}+\tau_{gi}^{rk}\epsilon_{ik}\right). \qquad (2.11)$$

In order for (2.11) to give a meaningful result, the double sum must be positive. This will be true provided the system of equations (2.9)

has coefficients which define a positive-definite matrix. Then it can be seen from either (2.8) or (2.11) that the estimate of analysis error, E_{gr}, is less than the root-mean-square error $\left(\overline{f_{gr}^2}\right)^{\frac{1}{2}}$ of the guess value by an amount which depends on the weights a_{ik} which the observations used in the analysis received. In the event that no observations are made in the vicinity of the grid point, the "analysis" error is just the error of the guess value.

Three kinds of correlation coefficient appear in the equations (2.9) for determining the observational weights. One of these, $\rho_{ij}^{k\ell}$, is the correlation of the error f_{ik} in the guess value at one location with the corresponding error $f_{j\ell}$ at another location. The specification of this correlation is discussed in the following section. Another correlation, $\eta_{ij}^{k\ell}$, is that of the observational error at one location with the observational error at another location. This correlation is discussed in Section 4.

The third correlation which appears in (2.9), $\tau_{ij}^{k\ell}$, is that of the error in the guess value at one location with the error in the observation at another location. Since conventional observations are usually made with no knowledge of the forecast or other guess value, $\tau_{ij}^{k\ell}$ is usually zero for them. Exceptionally, an error in the observing equipment (such as a bad baseline check for a rawinsonde) may be present for several consecutive observing periods and, since a forecast used as a guess depends on previously observed data, may lead to nonzero $\tau_{ij}^{k\ell}$. Certain types of remote sensors, in particular satellite radiometers, tend to produce "observations" which define smoother fields, with less amplitude, than exist in reality (Desmarais, et al., 1978). Forecast fields are similarly smoother than the true fields, thus the errors of these two quantities may well be spatially

correlated. The magnitude of this correlation, if any, has not been determined. We follow Gandin and Kagan (1974) and assume that the correlations $\tau_{ij}^{k\ell}$ are negligible, although we may not always be justified in doing so. With this simplification, (2.9) and (2.11) become

$$\sum_{\ell=1}^{m} \sum_{j=1}^{n_\ell} \left(\rho_{ij}^{k\ell} + \eta_{ij}^{k\ell}\epsilon_{ik}\epsilon_{j\ell}\right) a'_{j\ell} = \rho_{ig}^{kr}, \qquad k = 1,2,\ldots,m;\ i = 1,2,\ldots,n_k; \quad (2.12)$$

and

$$E_{gr}^2 / \left(\overline{f_{gr}^2}\right) = 1 - \sum_{k=1}^{m} \sum_{i=1}^{n_k} a'_{ik}\rho_{ig}^{kr}. \quad (2.13)$$

3. Determination of error correlations of the guess, or background, field

As stated previously, the NMC global analysis program analyzes temperature and the two horizontal wind components multivariately. Hence both auto-correlations of these variables and cross-correlations between them must be specified. We choose to impose a geostrophic constraint, in the form of the thermal wind equation, between errors of the temperature and wind component guess fields. A more realistic constraint could be imposed, but the geostrophic constraint has the virtues of simplicity of formulation and of proven satisfactoriness in multivariate optimum interpolation analysis (Rutherford, 1976; Schlatter, et al., 1976).

Let t, u, v represent the corrections to be made to the background fields of temperature and the horizontal wind components respectively. In other words, let t_i, u_i, and v_i be the f_{ik} of (2.4) and following equations.

They are assumed to be interrelated as follows, in Cartesian coordinates:

$$\left(\frac{\partial u}{\partial p}\right)_i = \frac{G_i R}{f_i p_i}\left(\frac{\partial t}{\partial y}\right)_i \tag{3.1}$$

$$\left(\frac{\partial v}{\partial p}\right)_i = \frac{G_i R}{f_i p_i}\left(\frac{\partial t}{\partial x}\right)_i \tag{3.2}$$

Here G is a "coefficient of geostrophy" as defined by (3.20), R is the specific gas constant for air, f is the Coriolis parameter, x and y are horizontal location coordinates described in the next paragraph, and p the pressure altitude of the point i.

The horizontal coordinates x_i and y_i of an observation or grid point are defined in terms of its latitude ϕ_i and longitude λ_i as follows:

$$x_i = A\, m_i \cos\phi_i \cos\lambda_i, \tag{3.3}$$

$$y_i = A\, m_i \cos\phi_i \sin\lambda_i, \tag{3.4}$$

where A is the radius of the earth, and in the Northern Hemisphere,

$$m_i \equiv \frac{2}{1 + \sin\phi_i}$$

is the map factor, true at the North Pole, for a polar stereographic projection. In the Southern Hemisphere, the map factor is defined by

$$m_i \equiv \frac{2}{1 + \sin(-\phi_i)} .$$

In each hemisphere, the approximate true earth distance is then given by

$$\Delta s_{ij} = \frac{2}{m_i + m_j}\left[(x_i - x_j)^2 + (y_i - y_j)^2\right]^{\frac{1}{2}} \tag{3.5}$$

If points i and j lie on opposite sides of the equator, either the Northern or Southern Hemisphere definitions of m_i and m_j and corresponding definitions of x_i, y_i, x_j, y_j, are used but not both. Definitions of u_i, v_i, u_j, v_j correspond in orientation with positive x_i, y_i, x_j, y_j.

Although the analysis is actually performed at latitude/longitude grid points in order to provide initial conditions for the NMC global model, it is convenient to work with distances, directions, and velocity components in cartesian coordinates on a polar stereographic grid because the correlation functions given below and in the appendices then assume their simplest form.

If (3.1) and (3.2) apply, then it may be shown that the covariances* between two points, i and j, of the variables t, u, and v are as a consequence related as follows:

$$\frac{\partial}{\partial \ln p_i}\left(\overline{u_i t_j}\right) = \frac{G_i R}{f_i}\frac{\partial}{\partial y_i}\left(\overline{t_i t_j}\right) \tag{3.6}$$

$$\frac{\partial}{\partial \ln p_j}\left(\overline{t_i u_j}\right) = \frac{G_j R}{f_j}\frac{\partial}{\partial y_j}\left(\overline{t_i t_j}\right) \tag{3.7}$$

$$\frac{\partial}{\partial \ln p_i}\left(\overline{v_i t_j}\right) = -\frac{G_i R}{f_i}\frac{\partial}{\partial x_i}\left(\overline{t_i t_j}\right) \tag{3.8}$$

$$\frac{\partial}{\partial \ln p_j}\left(\overline{t_i v_j}\right) = -\frac{G_j R}{f_j}\frac{\partial}{\partial x_j}\left(\overline{t_i t_j}\right) \tag{3.9}$$

$$\frac{\partial^2}{\partial \ln p_i \partial \ln p_j}\left(\overline{u_i u_j}\right) = \frac{G_i G_j R^2}{f_i f_j}\frac{\partial^2}{\partial y_i \partial y_j}\left(\overline{t_i t_j}\right) \tag{3.10}$$

$$\frac{\partial^2}{\partial \ln p_i \partial \ln p_j}\left(\overline{v_i v_j}\right) = \frac{G_i G_j R^2}{f_i f_j}\frac{\partial^2}{\partial x_i \partial x_j}\left(\overline{t_i t_j}\right) \tag{3.11}$$

$$\frac{\partial^2}{\partial \ln p_i \partial \ln p_j}\left(\overline{u_i v_j}\right) = -\frac{G_i G_j R^2}{f_i f_j}\frac{\partial^2}{\partial y_i \partial x_j}\left(\overline{t_i t_j}\right) \tag{3.12}$$

$$\frac{\partial^2}{\partial \ln p_i \partial \ln p_j}\left(\overline{v_i u_j}\right) = -\frac{G_i G_j R^2}{f_i f_j}\frac{\partial^2}{\partial x_i \partial y_j}\left(\overline{t_i t_j}\right) \tag{3.13}$$

---

*Strictly speaking, $\mathrm{Cov}(a,b) = \overline{ab} - \overline{a}\,\overline{b}$, thus the barred quantities in (3.6) through (3.13) are covariances only if $\overline{u}_i = 0$, $\overline{t}_j = 0$, etc. This is likely to be approximately true for a large statistical sample, but the analysis scheme does not require that such be exactly the case.

We next assume that the three-dimensional covariances $\overline{t_i t_j}$, $\overline{u_i t_j}$, etc., may be represented by analytical functions of the spatial coordinates; moreover that they may be expressed as the product of a quasi-horizontal function (at constant pressure) and a vertical function, i.e.,

$$\overline{t_i t_j} = \psi_{ij}^{tt}(x_i, y_i; x_j, y_j)\chi_{ij}^{tt}(p_i, p_j) \tag{3.14}$$

$$\overline{u_i t_j} = \psi_{ij}^{ut}(x_i, y_i; x_j, y_j)\chi_{ij}^{ut}(p_i, p_j) \tag{3.15}$$

and similarly for the other three-dimensional covariances. This assumption may be criticized on the grounds that it tends to make the analyzed fields of corrections more barotropic than would be the case if fully three-dimensional covariances were used. However, the direction and magnitude of the slope of baroclinic systems (and presumably also corrections to baroclinic forecasts) show a large variation in the atmosphere; any covariance function which was based on the "average slope" of systems would give misleading results in a large number of cases. Additionally, the factoring of the covariance functions into horizontal and vertical functions greatly simplifies their use in the analysis scheme.

If (3.14), (3.15), etc., are assumed, it is then possible to show that all of the other ψ-functions can be expressed in terms of ψ_{ij}^{tt} and that all of the other χ-functions can be expressed in terms of χ_{ij}^{uu}. These functions

may also be normalized to give the equivalent of correlation functions: μ_{ij}^{tt}, μ_{ij}^{ut}, etc., corresponding to ψ_{ij}^{tt}, ψ_{ij}^{ut}, etc., and ν_{ij}^{tt}, ν_{ij}^{ut}, etc., corresponding to χ_{ij}^{tt}, χ_{ij}^{ut}, etc. The mathematical details are given in Appendix A. Thus, if μ_{ij}^{tt} and ν_{ij}^{uu} are specified as differentiable functions of x_i, y_i, x_j, y_j (or alternatively λ_i, ϕ_i, λ_j, ϕ_j) and p_i, p_j respectively, then all of the other μ- and ν-correlations are automatically specified if the thermal wind relations (3.1) and (3.2) are valid. The total correlations are then given by

$$\rho_{ij}^{tt} = \mu_{ij}^{tt}\, \nu_{ij}^{tt}, \tag{3.16}$$

$$\rho_{ij}^{ut} = \mu_{ij}^{ut}\, \nu_{ij}^{ut}, \tag{3.17}$$

etc., and their use in (2.12) permits the deviations of the observed winds from their guess, or background, values to influence the temperature analysis to some extent, and vice versa.

There is a considerable literature on the form of the constant pressure correlation function for geopotential height residuals. A normal distribution form is used by Rutherford (1973, 1976) and Schlatter (1975) in their multivariate analysis schemes. Alternative forms are suggested by Thiebaux (1975, 1976) and by Julian and Thiebaux (1975). We have followed Rutherford and Schlatter and used

$$\mu_{ij}^{tt} = \exp[-k_h(\Delta s_{ij})^2], \tag{3.18}$$

where k_h is a constant with dimensions $[\ell^{-2}]$, and Δs_{ij} is given by (3.5), for the isobaric correlation function of temperature residuals, which is thus assumed to be isotropic and the same as that for geopotential height. The latter assumption is supported by (27B) of Appendix B. Some preliminary statistical evidence (Bergman and Gordon, 1977) on the isobaric

component of the temperature auto-correlation indicates that (3.18) with $k_h = .98 \times 10^{-6}$ km^{-2} models it reasonably well. Isopleths of this correlation and of the other μ-correlations derived, in Appendix A, from (3.18) are shown for 45°N latitude in Fig. 1. These patterns are essentially the same as the geopotential height and the wind correlations of Rutherford (1973, 1976) and Schlatter (1975). They are also supported approximately by the forecast-error correlation statistics which have been accumulated thus far at NMC.

The form currently assumed for the vertical auto-correlation of the u wind component is

$$\nu_{ij}^{uu} = \frac{1}{1 + k_p \ell n^2 (p_i/p_j)} , \tag{3.19}$$

where $k_p = 5.0$. This form was obtained from preliminary vertical auto-correlation statistics for the wind components which, except for the 1000 mb correlations with other levels, showed approximate independence of the statistical correlation profile with respect to the specific pressure level p_i. Later statistics (Bergman and Gordon, 1977) indicate that a larger value of k_p may be appropriate, but the value used in the analysis scheme was not changed for the experimental runs discussed here. The ν_{ij}^{vv} auto-correlation is assumed equal to the ν_{ij}^{uu} auto-correlation in the analysis scheme, and this assumption is well justified by the available correlation statistics. The ν-correlation functions are derived in Appendix A and shown in Fig. 2.

As shown by (36A) through (40A) of Appendix A, with the given choice of correlations (3.18) and (3.19), the mean square error of the guess temperature field, $\overline{t_i^2}$, is a constant, and the corresponding wind component errors, $\overline{u_i^2}$ and $\overline{v_i^2}$, are equal and a function of latitude only. Essentially, this is a result of assuming that (22A) and (23A), the covariance counterparts of (3.18) and (3.19), are both homogeneous functions, independent of specific x,y,p location in the atmosphere and dependent only upon the difference between the two points involved.

Actually, the mean square errors of the numerical predictions used for the guess fields vary both laterally and with pressure. Statistics compiled by Dey and Caporaso (1979) show that the rms temperature error varies laterally by a factor of approximately 2, and the rms vector wind error by approximately 3, between the Northern Hemispehre continents and the Southern Hemisphere oceans. Values of forecast error standard deviation are shown in Table 1 as a function of pressure. Both the former and the latter values were obtained by comparing 6-hr forecasts produced by the global model with rawinsonde observations.

In practice, the analysis scheme assumes "local homogeneity," both laterally and vertically, of the correlation functions and the implied variances for all forecast errors in the vicinity of the grid point and pressure level being analyzed. Since the maximum lateral distance between an observation used for the analysis at a grid point and the grid point itself is 15° latitude, the assumption of lateral homogeneity is probably not a serious problem. Similar lateral homogeneity assumptions are made

by Schlatter (1975) and Rutherford (1976) in their analysis schemes. The assumption of vertical homogeneity may seem more questionable in view of the variability of the forecast errors shown in Table 1, but in practice data displaced more than 2 mandatory levels away from the analysis level are rarely used in analysis because the correlations at greater separations are so small (Fig. 2). The equating of $\overline{u_i^2}$ and $\overline{v_i^2}$ is supported by Table 1.

It is possible to define factored covariance and correlation functions which imply spatially variable variances, at least in the vertical, but such functions have not been tried in the NMC analysis scheme.

measurements and, in general, the errors of observations from differing observing systems are uncorrelated. Also, the errors of measuring two different meteorological variables, even if measured by the same instrument, are unlikely to be correlated. An example is temperature and the u-component of wind, both measured by the same rawinsonde. (Errors of the u- and v-components of wind are uncorrelated provided the measured errors of speed and direction are uncorrelated.)

The situation is different for a time sequence of observations taken by the same instrument. An error in an observation at one time is likely to be related to the error at a proximate time. The available evidence on observational errors bears this out. Rawinsonde observations at two adjacent pressure levels using the same instrument are found to have correlated errors (Hollett, 1975) for both temperature and wind components. The temperature observations obtained from satellite radiance measurements have errors which are correlated horizontally along a satellite orbital path (Bergman, 1978; Schlatter and Branstator, 1978). Because of the way the vertical temperature profiles are constructed from the radiance measurements, it is likely that these temperature errors are correlated vertically too, although the evidence is conflicting (Bergman, 1978). For other observing systems in use at the present time, observations are not likely to have significantly correlated errors, and we have so assumed in the analysis scheme until evidence to the contrary is available.

In the analysis scheme described here, the vertical error correlations of rawinsonde temperatures and winds, and of satellite temperatures, are modeled with the functions shown in Fig. 4. The rawinsonde values were obtained by fitting curves of the form of (3.19) to Hollett's values of error correlation between mandatory pressure levels, and the satellite values from comparison with an analysis by C. Hayden (unpublished manuscript). The horizontal correlation of satellite temperature errors is modeled with a function of the form (3.18) except that $k_h = 11.3 \times 10^{-6}$ km^{-2}. This value was obtained by fitting a curve to the Nimbus error correlation statistics obtained by P. Polger and J. Horodeck of NMC as shown in Fig. 5. Similar horizontal error correlation statistics have been obtained by Schlatter and Branstator (1978).

5. Determination of observational errors

Finally, the normalized observational error standard deviations (the ε's of (2.12) must be specified for each type of observation and instrument. The values given in Table 2 were used for the experimental analyses discussed in this paper. These values are assumed to be independent of spatial and temporal location, although it is recognized that this is an oversimplification. A more realistic treatment of observational errors appears in the companion paper (McPherson et al., 1979), wherein the errors of the forecast field used as a "first guess" are allowed to evolve in space and time through cycling of the analysis-forecast routine on itself.

Note that the error characteristics of many of the observing systems, old as well as new, are known only very approximately at best. Studies are in progress at NMC (Bergman, 1978) and elsewhere to improve the estimates of some of these observational errors.

6. Use of surface observations in upper air analysis

Surface observations are incorporated in the upper air analysis in the following way. Surface pressure residuals (differenced between observed surface pressure and guess surface pressure) are converted to equivalent geopotential height residuals by the following approximate relation:

$$z_1 \simeq \frac{\overline{RT}}{g} \frac{p_o}{\tilde{P}_o}, \tag{6.1}$$

where z_1, is the equivalent height residual at pressure level P_1, $\overline{T}$ is the mean temperature of the layer between the surface pressure P_o and level P_1, p_o is the observed surface pressure residual, and $\tilde{P}_o$ is the guess value of surface pressure at the observing site. Thus far, we have used only ship surface pressure observations for which we can set $\overline{T} \simeq T_o$, the surface temperature. Otherwise, it is necessary to make an assumption about the thermal lapse rate between the surface and level P_1.

Assuming that the geostrophic and thermal wind relations hold between the residuals of geopotential height and the temperature and wind component residuals, it is shown in Appendix B that all of the new correlations between height and the other residuals are expressible in terms of the multivariate (t,u,v) correlations already derived in Appendix A. Thus,

The thermal wind balancing implied by (3.1) and (3.2) is obviously not applicable in the immediate vicinity of the equator. Thus, it is necessary to gradually decouple the temperature and wind analyses as the equator is approached. This is accomplished by means of the coefficient of geostrophy G, a function of latitude.

In order to estimate the profile of this function, a brief study of the geostrophicity of the wind in the tropics was conducted. A month's worth of data for stations between 5°N and 35°N latitude was sorted into three latitude bands (5°N-15°N, 15°N-25°N, 25°N-35°N) and the mean ratio of (V/V_G) computed for each latitude band. This was done by computing the mean component of wind speed normal to the line connecting pairs of observing stations and comparing this speed with the geostrophic speed computed from the height gradient along the line connecting the stations. Certain restrictions were imposed on the data, namely that the stations be separated by distances between 2° and 5° latitude, that the wind directions at the two stations be within 90° of each other, and that the speeds of the normal components at the two stations be within 50 percent of each other. The computations were done for winds at 850, 500, and 200 mb. As there was comparatively little variation in the ratio (V/V_G) with pressure, the results for the three levels were combined and are plotted in Fig. 3 for the three latitudinal bands. Assuming that this coefficient of geostrophy vanishes at the equator and approaches unity at high latitudes, a functional form

$$G \equiv V/V_G = 1 - \exp(-.05|\phi|), \tag{3.20}$$

where ϕ is the latitude in degrees, was fitted to the three plotted values. This function appears in the observational scaling factors of (2.10e) and has the effect of reducing the amount of correction made to one variable field by cross-correlated observed residuals of another variable field.

The role of cross-correlated corrections to the analyzed fields is worth discussing in more detail. First, it should be noted that, since only corrections to the guess, or background, field are made using the geostrophic thermal wind relation, any ageostrophic component of a guess field will be found, to some extent, in the final analysis. Second, the role of the geostrophy function, G, in reducing the magnitude of cross-correlated corrections has just been noted. Finally and most importantly, in practice the analysis is univariate, or nearly so, in those areas where a fairly dense data coverage including both temperature and wind measurements exists. The multivariate capability of the analysis scheme is utilized primarily in those regions where data are sparse, or where data of one type are not complemented by data of the other types. An example is satellite temperature data in oceanic areas where no wind data are available, in which case the u and v wind component analyses will be adjusted by geostrophic corrections corresponding to the implied thermal gradients of the satellite data.

4. Determination of observational error correlations

It has been shown by Gandin et al.(1972), Bergman and Bonner (1976), and Seaman (1977) that the correlation of the errors of neighboring observations affects the net informational content of them. When observational errors are positively correlated with each other, the informational content is

reduced for the observed variable but enhanced for the gradient of that variable. Thus, it is important that the error correlations, if non-zero, be specified in order for these observations to receive proper weight in the interpolation process.

For many pairings of observations, we may safely assume that the observational errors are completely uncorrelated. Thus, rawinsonde temperature measurements do not depend in any way on satellite temperature

the P_1-level height residuals may be used in the temperature and wind component analyses provided their weights are scaled as indicated by (2.10è). In practice, we have set P_1 = 1013.2 mb.

Ship wind reports are included in the data base for the analyses after being adjusted to approximate equivalent geostrophic values. The adjustments are obtained from Druyan (1972) for the case of neutral static stability and are

$$U_G = 1.91\ U - 5.97, \tag{6.2}$$

with U_G not permitted to be less than zero, and

$$\Delta\theta = -\ 17.3(U/U_G) + 26.5 + 0.04(L - 35), \tag{6.3}$$

where U is the ship wind speed in knots, U_G is the equivalent geostrophic wind speed in knots, L is the latitude in degrees, and $\Delta\theta$ is the inflow angle correction in degrees. These expressions for adjustment are based on V. Cardone's 1969 model of the marine boundary layer which relates the actual wind at 19.5 m to the sea-level geostrophic wind. This adjustment seems to work reasonably well in practice, and it is also used in the multivariate analysis of surface pressure and winds (McPherson et al., 1979).

The vertical correlation function (3.19) which is also used for the vertical correlation of Z decreases fairly rapidly in magnitude with increased vertical separation; thus, the ship pressures and winds affect the analysis mostly in the lower layers and have virtually no impact on the analysis above 700 mb.

7. Some design aspects of the NMC global scheme

a. Data search and selection procedure

A preanalysis program sorts the observed data by latitudinal strips, and then by longitude within each strip. The data are not sorted by level.

The observation residuals are computed by linear interpolation of the guess field from the longitude-latitude grid to the horizontal positions of the observations, and by linear interpolation in the logarithm of pressure from the prediction layers of the forecast model to the pressure levels of the observations.

A search is made of the data about each grid point to be updated. Successive boxes of approximately 15^{o}, 20^{o}, 25^{o} and 30^{o} latitude on a side, centered on the grid point, are scanned until the following criterion is met: A combination of complete radiosonde and satellite soundings is required which adds up to 6, with each rawinsonde counting as 2 and each satellite sounding counting as 1. When either this condition is satisfied or the largest box has been scanned, the search stops, and the correlations between the variable being analyzed at a grid point/level and each observation within the largest box scanned, i.e., the correlations appearing on the right side of (2.12), are determined. Note that cross-correlations between variables as well as auto-correlations are computed. To allow for the variable quality of observations, each correlation is divided by $(1+\varepsilon^2)$, where ε is the assumed normalized error standard deviation of the observation. This procedure is done separately for each pressure level at the grid point for which an analyzed value is desired, and it is done

separately for each of the variables to be analyzed. The 10 observations with the highest resulting values in each case are used to perform the interpolative analysis. The choice of 10 is arbitrary; Belousov et al. (1972, pp. 101-102) indicates that using five to eight observations may be sufficient in most cases. If fewer than 10 observations are above the assigned threshold correlation of 0.1, all are used; if there are no observations with correlation above this threshold, the guess value remains unaltered by the analysis routine.

The above procedure selects the observations used in the analysis solely on the basis of their correlation with the variable to be analyzed at the grid point and level, with allowance for observational error. The inter-observational correlations are neglected, and thus there is no guarantee that the 10 observations selected are necessarily the 10 observations which would receive the largest weight should all observations be used in the analysis. An alternative procedure would be to do stepwise regression on a larger set of observations than those actually used, but this would be computationally expensive.

The effect of large inter-observational correlations between closely positioned observations is to reduce the effective information content of these observations, and hence the weight as determined by (2.12) that each receives in determining the grid point correction. In an effort to correct approximately for this, an alternative version of the analysis was run with all cross-correlations augmented by an empirically determined 75 per cent in the selection procedure only. This allows observations which are

cross-correlated with the grid point, and usually at some distance from either the grid point or other observations (hence only weakly correlated with them), to be selected in preference to auto-correlated observations, which are usually clustered close to the grid point and to each other in areas of dense data coverage. This procedure generally resulted in improved analysis, as measured by a reduced estimated analysis error, in data-dense areas. In fact, various augmentations of the cross-correlations were tried, and 75% produced the lowest estimated analysis error, given by (2.13), overall.

The data selection process is the most arbitrary aspect of the entire analysis method, and it is in need of improvement provided such improvement can be made without appreciably increasing machine time.

b. Computation of observational weights

Once the correlations and the normalized observational errors of (2.12) have been specified for the set of observations used to obtain an analyzed value at a specific grid point and level, these linear equations may be solved for the observational weights a'_{jl}. Since the left-side matrix of coefficients may be ill-conditioned for certain distributions of observations relative to the grid point, we have chosen not to perform matrix inversion but rather to use an iterative scheme, the method of conjugate gradients (e.g., Beckman, 1960). A similar iterative method, steepest descent, is used successfully in the Canadian analysis scheme (Rutherford, 1976). Convergence with the conjugate gradient method is usually rapid. Ill-conditioned cases still occasionally lead to non-convergence, a situation that usually is corrected by averaging the pair

of observations which are most highly correlated with each other. However, the number of cases where this occurs is a very small percentage of the total.

The weights $a'_{j\ell}$ thus obtained are converted to the weights $a_{j\ell}$ by means of the definition (2.10c). The analyzed value of the variable r at grid point/level g is then obtained with (2.5). When the observed variable and the analyzed variable are the same, the scaling factor of eqn. (2.10e) is equated to unity, equivalent to assuming that the variance $\overline{f^2_{j\ell}}$ of the variable is constant in the vicinity of a particular grid point and level, although it may change when the analysis shifts to another grid point or level.

The normalized estimate of analysis error, eqn. (2.13), is also computed once the a'_{ik} have been determined. Its value, which depends solely on the physical locations of the observations and the assumed correlation among them, lies between zero and one. The smaller the normalized estimated error, the more strongly the analysis has weighted the observations relative to the guess value f_{gr} in determining the analyzed value. Since none of the observations are ever assumed completely error-free, the normalized error estimate can never be zero even in the event of an observation at precisely the analysis grid point and level. If, on the other hand, no observations are significantly correlated with the grid point/level, the guess value remains unaltered and the normalized error estimate is unity.

c. Data quality control

The observational data base for the analysis is subjected to two error-checking routines in order to remove bad or unrepresentative observations. The first of these is a gross error check, done after the observation-minus-forecast residuals are computed but before the analysis routine is entered. A residual is rejected if it is excessively large, i.e., differs from the forecast by an improbably large amount. The gross rejection limits are a function of latitude and are quite liberal, erring in the direction of accepting bad observations at this point rather than risking the rejection of good ones.

Subsequently, within the analysis routine, each observation is compared with its neighbors of like kind. If an observation is too inconsistent with its neighbors, it is labeled "bad" and rejected. This comparative check is done in the following way: The correlations $\rho_{ij}^{k\ell}$ between all possible pairs of observations used for the analysis at a particular grid point are computed in the analysis routine in order to solve the system of equations (2.12) for the observational weights. These correlations are also used to do the comparative check. For each pair of residuals of the same meteorological variable, the following inequality is required to hold:

$$|\hat{f}_i - \hat{f}_j| \leq (a - b\rho_{ij}^{kk})\sigma \qquad (7.1)$$

where a and b are empirical constants (currently a = 6, and b = 3), and σ is the forecast error standard deviation for the level at which the observations are located. Values of σ currently used are given in Table 1. If condition (7.1) is not met, the observations with the presumed lower quality is flagged; if both observations are of the same presumed quality, both are flagged. Presumed quality is currently determined for rawinsonde soundings only, on the basis of vertical consistency checks.* Depending on the outcome of this check, a quality indicator is assigned to each rawinsonde observation. Other kinds of observations are assigned a quality lower than that of the acceptable rawinsonde observation, and rawinsonde observations can only be flagged by other rawinsonde observations of equal or higher quality.

After all comparisons have been made, the total number of flags assigned each observation is determined, and the observation with the greatest number of flags is rejected first, provided that the number of flags is at least two. (If there is more than one observation with the greatest number of flags, they are both rejected.) Any flags which the rejected observation caused to be placed against other observations are removed, and the process is repeated until all remaining observations

---

*Quality indicators will be appended to satellite data produced by the National Environmental Satellite Service (NESS) during the Global Weather Experiment.

have no more than one flag. This procedure requires that two or more observations of equal or better quality must be in disagreement with an observation in order for it to be rejected, and it insures that bad observations are not allowed to reject good ones. It works well in practice. An example of the method is given by Bergman (1978). The comparative check is done separately at each grid point, so it is possible for an observation to be accepted for the analysis at one grid point and rejected at a neighboring grid point, but the actual instances of this are few, occurring when the accepted observation is peripheral to the grid point and receives a very small weight in the analysis.

8. An example of multivariate analysis

Figures 6, 7, 8, and 9 illustrate the multivariate analysis of temperature for the 500-mb level at a grid point in the North Atlantic. Figure 6 shows the guess, or background, temperature field used for this analysis. In this case it was a 24-hour forecast of 500-mb temperatures valid at the analysis time of 0000 GMT 9 February 1975. The illustrative grid point is at 50°N latitude and 40°W longitude.

Figure 7 shows the 10 observed quantities selected by the routine to update the T_{500} analysis at 50°N/40°W. Note that one u-component and two v-components of wind are used in the analysis, and that they are selected from levels other than 500 mb. This is a result of the vertical part of the cross correlations, ρ_{ij}^{ut} and ρ_{ij}^{vt}, having maxima or minima at

pressure levels other than 500 mb as shown in Fig. 2. The numbers in parentheses are the relative weights (the a_{ik}' of (2.13)) which each observation receives. (2.13) gives a value of 0.60 for the ratio $E_{gr}/(\overline{f_{gr}^2})^{\frac{1}{2}}$. The interpretation is that the estimated analysis error is 60 percent of the assumed error in the forecast temperature for this grid point and level.

After the weights are scaled according to (2.10e), the analyzed temperature correction as given by the right-hand term of (2.5) is found to be 4.5°C. This is shown in Fig. 8 along with the field of algebraic temperature corrections for the surrounding North Atlantic area. Finally, addition of these corrections to the background field yields the updated analysis of Fig. 9. The temperature data observed at 500 mb is plotted for comparison. However, it should be remembered that the 500-mb temperature data do not comprise all of the data used in the analysis. Note that the isotherms fit the rawinsonde temperatures more closely than the satellite temperatures, a result of the higher levels of rms error and error correlation assigned to the satellite data.

Another example of the data selected for analysis of a grid point/level is shown in Fig. 10. Here, the 500-mb u-component of wind is updated at 50°N/40°W by the indicated observed data. Weights are again in parentheses. Note the use of two temperature observations multivariately in the wind analyses. In this case, (2.13) indicates that the estimated analysis error is 82 percent of the assumed forecast error.

In practice, the temperature analysis is univariate and the wind component analyses either univariate or bivariate (in u,v) in regions where data of each type exists with sufficient density. Such is generally the case over the continents of the Northern Hemisphere. In these regions, any balance which exists between the mass and momentum fields is determined by the data themselves. The full multivariate capability of the analysis scheme is used only in those areas where data are sparse or limited to one kind only. For example, there may be abundant satellite temperature data but no wind data in some oceanic areas. In the latter case, a geostrophic adjustment is made to the momentum field to preserve a degree of balance with the newly adjusted mass field. Otherwise, studies indicate that the effects of adjusting the mass field alone are largely dispersed in gravity waves (Kistler and McPherson, 1975).

The lack of geostrophic adjustment imposed by the analysis scheme in regions of dense, complete data coverage is believed to be a desirable feature. It is better for the balance which exists in these areas to be specified by the data in conjunction with the background field rather than by an overly restrictive geostrophic constraint. On the other hand, the analysis profits in data-limited regions from geostrophic adjustment in place of no mutual adjustment at all.

9. A discussion of experimental analysis results

A series of experimental analyses were performed using the scheme described above. The results are summarized in Table 3. The data base

for these analyses consisted of observations within 3 hours of 0000 GMT 3 December 1977, and the background field was provided by a 6-hour forecast using the NMC global model (Stackpole et al., 1974) in its nine-layer version. This forecast was selected from the middle portion of a global data assimilation cycling experiment (McPherson et al., 1979) with updating performed every 6 hours by optimum interpolation.

For the present study, only the 500-mb analysis of temperature and wind components was performed on a longitude-latitude grid of 5^{o}. However, the data search was three-dimensional; some data at other pressures were used in the 500-mb analysis. The analysis was restricted to the Northern Hemisphere.

The numbers of Table 3 allow comparison in two ways. The first of these is the normalized estimate of analysis error; that is, the square root of the quantity given by (2.13). The second is the root-mean-square "fit" of the analysis, after linear interpolation to the locations of the observations, to the data. The latter number should emphatically not be used as an exclusive measure of the "goodness" of an analysis! A reasonable degree of agreement between analysis and observations is to be expected, of course, but it must be remembered that the observations have been labeled "imperfect" and assigned error characteristics in the analysis scheme. Thus, the analysis does not attempt to fit the data exactly. Recall that the background field (the forecast) is assumed to have some skill, hence it also has some weight in the final analysis, the more so where the observations are scattered or are of

questionable quality. This point cannot be emphasized too strongly, since the natural tendency of the uninformed person is to judge the quality of an analysis solely on the basis of its rms fit to the data.

The normalized estimate of analysis error, while useful, is by no means a definitive measure of analysis quality either. Since it is only an estimate based upon the distribution and type of observations, it will be misleading when (1) the assumed statistical error characteristics have been specified incorrectly or (2) the unknown actual errors of the individual observations differ markedly from the assumed statistical values. One can argue that, for a large ensemble of grid point analyses, the latter problem will be minimized when computing average values, but the former inaccuracy may still be present. The specification of observational error characteristics admittedly is somewhat crude in the present scheme, and improvement is desirable. However, some evidence given below suggests that the analysis results are not unduly sensitive to the exact specification of error characteristics.

Other ways to evaluate the relative quality of analyses are (1) making numerical predictions from the initial conditions defined by the analyses and comparing their performances, and (2) using diagnostic methods such as those of Krishnamurti (1968) and Stuart (1974) to evaluate the analyses. The first of these is open to the criticism that the errors of an analysis are combined with the errors of the prediction model, and that the "best" analysis selected by one prediction model may not be the best in terms

of another model. This suggests that the analysis and prediction methods should be designed as a cohesive pair at centers, such as NMC, where forecasts are the primary end product.

With the above caveats in mind, we may proceed with a discussion of Table 3. Run A is a null-analysis showing for comparison the rms fit to the data of the forecast used as the background field. Runs B and C show the comparison between the unaugmented and the augmented cross-correlations in the selection procedire as described in Section 7a. It was found experimentally that neither the estimated analysis errors nor the rms differences varied significantly for augmentation up to 1.75, but that both increased markedly for augmentation of 2.0 or greater. Examination of analyses produced by Runs B and C shows little difference between the two in most areas.

Comparison of Run B or C with D shows that complete decoupling of the temperature and wind analyses results in very small changes in the statistics. The only significant difference is in the normalized estimated analysis error for temperature, where some improvement is indicated for the multivariate analyses over the univariate one. This result is consistent with Schlatter's (1975) conclusion that the mass analysis is improved by use of wind information, but that the momentum analysis is not improved by the use of mass information. Rutherford (1973) shows an improvement in 12-hr height forecasts made from multivariately analysed height and wind fields over those made from decoupled fields even though the rms deviations of the analyses from the observed data were virtually the same in both cases. We may surmise that,

in the fully multivariate case, the mass field may be in more realistic balance with the momentum field, leading to improved forecasts.

The difference in the normalized estimated temperature error between Runs C and D is slight and comparison of the two temperature analyses shows only small, subtle differences in some oceanic areas. Since the maximum permissible cross-correlation between a temperature and wind residual is only 0.28, then, even when cross-correlated observations are selected, they are likely to receive small weights compared to auto-correlated data or the background field.

Although individual cross-correlated observations may receive little weight in the analysis of a grid point/level, the possibility exists that if enough of them are selected, their combined weight may be appreciable. In order to see whether the restriction to a maximum of 10 observations operates against sufficient combined weight assigned to cross-correlated observations, Runs E and F were made with a maximum of 20 observations. Here, it can be seen that the difference in the normalized estimated temperature error is greater than between Runs C and D. This result suggests that the use of more observations results in some improvement in the analysis, probably because the cross-correlated observations receive greater combined weight. However, note that the rms differences are larger for 20 observations than for 10 observations, although the reverse is true for the normalized estimated errors.

In Section 7a, it was mentioned that the choice of 10 observations as the maximum was arbitrary. Runs G and H, with 6 and 8 maximum observations respectively, investigate the feasibility of using fewer observations. Comparison of these runs with Run C (10 observations) and Run E (20 observations) indicates that the normalized estimated errors decrease as the maximum number of observations increases, a result implied by (2.13), but the rms differences show a slight tendency to increase. The optimum number of observations is not clearly indicated by these results.

Run I used only wind data in the temperature analysis, and only temperature data in the wind analysis. The normalized estimated errors show that the improvement in the analysis is small (compare Run A) but is somewhat greater for the temperature analysis than for the wind analysis. This result indicates in another way that the ability of cross-correlated data to improve the analysis is small at most grid points.

Runs J and K investigate the sensitivity of the analyses to changes in the rms errors assigned to the observations. In Run J, the values of Table 1 are divided by 2; in run K, these numbers are multiplied by 2. In Table 3, the normalized estimated analysis errors are placed in parenthesis since they cannot be compared directly with values from other runs. (Recall that these estimates assume that the error levels have been correctly specified. They merely give an estimate of the minimum analysis error achievable when the assigned observational error levels are valid.) Comparison of the rms fits of the analyses to the observations for Runs J and K indicate that changing the assigned rms observational errors by a factor of 4 does not change the rms fit by a

large amount. Comparison of the analyzed residual fields themselves (not shown) indicates close agreement of the patterns of correction, but with the magnitude of the Run J residuals averaging about 50 percent greater than those of Run K. This is the expected result; the smaller assigned observational rms errors of Run J give the observations more weight in making adjustments to the background fields. We conclude that the analysis routine is moderately, but not extremely, sensitive to the observational rms error values.

Finally, Runs L and M test the sensitivity of the analyses to changes in the horizontal correlation of errors in the background field. In Run L, the value of k_h in (3.18) has been reduced by a factor of 4 to $.24 \times 10^{-6}$ km^{-2}. In Run M, k_h has been multiplied by 4 to become 3.92×10^{-6} km^{-2}. The μ^{tt} correlation of Run L thus has twice the half-width of that of Run C, whereas for Run M the half-width is half of Run C's. The other horizontal correlations are changed by like amounts.

The rms fits to the observations (Table 3) show a moderately strong dependence on the variation of the horizontal correlations. Comparison of the analyzed residual fields shows much broader, smoother correctional patterns with Run L than with Run M. Thus, the correct specification of the breadth of at least the horizontal correlations (and probably also the vertical correlations) appears to be of some importance. Experiments which vary the functional form of the correlations have not been performed at NMC; however, an experiment by Schlatter et al. (1977) suggests that statistical analysis schemes are not very sensitive to this factor.

The sensitivity of the analyses to variation of the correlation functions for errors of the background fields is important because we have determined these correlations only in a data-rich areas (North America) and have thus far assumed that these correlations apply everywhere on the earth. However, it is likely that the error correlations, as well as the rms error levels, of the background (forecast) fields are appreciably different in data-poor areas or in areas of lower quality data. Statistical computation of these correlations in such areas is made difficult by the characteristics of the data available, but it is hoped that they will be done in the future. Most likely, the correlation functions will prove to have greater breadth in these areas than in the North American rawinsonde network, since it is reasonable to suppose that larger forecast errors in the longer meteorological wave lengths will occur in the data-poor areas.

10. Summary

A multivariate optimum interpolation statistical analysis scheme for temperature and wind fields has been presented and illustrated by an example analysis. A series of experimental analyses have been compared, and the sensitivity of the analyses to variations in some of the parameters of the scheme has been discussed. The scheme is designed to periodically assimilate heterogeneous observed data into a continuing global numerical prediction, as described in the comparison paper.

The design of the multivariate analysis system is similar to those of Rutherford (1973, 1976) and Schlatter (1975), but differs in being explicitly three-dimensions, in incorporating geostrophy implicitly

with the thermal wind constraint, in having a more complete specification of observational error characteristics, and (in the experimental version) in explicitly including oceanic surface observations in the upper-air analysis.

The current procedure for selecting observations used in the analysis of a grid point/level has arbitrary features, and Section 7 points out that this is one of the weakest aspects of the entire analysis scheme. More logical ways of selecting observations are available, but they are currently too expensive to be feasible for an operational analysis system. Some future improvement in the selection procedure may be possible without exceeding operational time constraints.

The results of the experimental analyses indicate the following:

(1) The use of temperature-wind cross-correlations results in slight improvement of the temperature analysis but no significant change in the wind analysis.

(2) The use of temperature-wind cross-correlations has more impact on the temperature analysis if the maximum number of observations used is increased.

(3) Use of winds only in the temperature analysis, and vice-versa, results in analyses which show little improvement over the numerical prediction used for the background fields.

(4) The quality of the analysis is not very sensitive to changes in the maximum number of observations used, so long as that number is between 6 and 20.

(5) The analyses are only moderately sensitive to the levels of rms observational error specified.

(6) The analyses are strongly sensitive to the half-widths of the horizontal correlations of the errors in the predictions used for the background field.

In light of the first result, one may question the need for fully multivariate analyses. Although the total impact of winds on the temperature analysis is small, undoubtedly there is desirable improvement in the relationship between the mass and momentum fields at specific times and places. Since the mass field tends to adjust to the wind field for intermediate wave lengths in numerical prediction rather than the other way around (Williamson, 1973), and since use of temperature data in the wind analysis results in no overall improvement, it may be more efficient not to use temperature data in the analysis of the wind field.

The need for better specification of observational error characteristics has been mentioned. It appears, however, that slight errors in the rms specifications will not have undue impact on the performance of the analysis scheme.

Finally, the need to specify the correlations of errors in the background fields as a function of location and time is indicated. The present assumption that these correlations are globally unvarying undoubtedly compromises the performance of the analysis scheme to some extent in those areas, primarily oceanic, where the observed data are sparse or of poorer quality.

Acknowledgments. Discussions with Drs. Ian Rutherford and Thomas Schlatter were especially helpful in the earlier stages of designing the analysis system. Valuable suggestions were made at various points in the development by Drs. Ronald McPherson, William Bonner, and Norman Phillips, and by Mr. Robert Kistler. Comments transmitted by Professor L. S. Gandin to the author were most beneficial. Much of the computer programming was done by Mrs. Doris Gordon and Mr. Kistler. The care with which Mr. Eugene Brown drafted the figures and Mrs. Mary Daigle typed the manuscript is greatly appreciated.

Appendix A: Derivation of Correlation Functions for Multivariate Temperature and Wind Analysis

Starting with equations (3.6) through (3.13) of the text, assume, as in (3.14) and (3.15), that each of the three-dimensional covariances can be expressed as the product of a function of horizontal position and a function of pressure. Using this assumption in (3.6) through (3.13) and separating each of the resulting equations into equations in (x_i, y_i, x_j, y_j) and (p_i, p_j) leads to

$$\psi_{ij}^{ut} = \frac{G_i R}{f_i} \frac{\partial}{\partial y_i} \left(\psi_{ij}^{tt}\right) \tag{1A}$$

$$\psi_{ij}^{tu} = \frac{G_j R}{f_j} \frac{\partial}{\partial y_j} \left(\psi_{ij}^{tt}\right) \tag{2A}$$

$$\psi_{ij}^{vt} = -\frac{G_i R}{f_i} \frac{\partial}{\partial x_i} \left(\psi_{ij}^{tt}\right) \tag{3A}$$

$$\psi_{ij}^{tv} = -\frac{G_j R}{f_j} \frac{\partial}{\partial x_j} \left(\psi_{ij}^{tt}\right) \tag{4A}$$

$$\psi_{ij}^{uu} = \frac{G_i G_j R^2}{f_i f_j} \frac{\partial^2}{\partial y_i \partial y_j} \left(\psi_{ij}^{tt}\right) \tag{5A}$$

$$\psi_{ij}^{vv} = \frac{G_i G_j R^2}{f_i f_j} \frac{\partial^2}{\partial x_i \partial x_j} \left(\psi_{ij}^{tt}\right) \tag{6A}$$

$$\psi_{ij}^{uv} = -\frac{G_i G_j R^2}{f_i f_j} \frac{\partial^2}{\partial y_i \partial x_j} \left(\psi_{ij}^{tt}\right) \tag{7A}$$

$$\psi_{ij}^{vu} = -\frac{G_i G_j R^2}{f_i f_j} \frac{\partial^2}{\partial x_i \partial y_j} \left(\psi_{ij}^{tt}\right) \tag{8A}$$

and to

$$\chi_{ij}^{tt} = \frac{\partial}{\partial q_i} \left(\chi_{ij}^{ut}\right) = \frac{\partial}{\partial q_i} \left(\chi_{ij}^{vt}\right) \tag{9A}$$

$$\chi_{ij}^{tt} = \frac{\partial}{\partial q_j} \left(\chi_{ij}^{tu}\right) = \frac{\partial}{\partial q_j} \left(\chi_{ij}^{tv}\right) \tag{10A}$$

$$\chi_{ij}^{tt} = \frac{\partial^2}{\partial q_i \partial q_j}\left(\chi_{ij}^{uu}\right) = \frac{\partial^2}{\partial q_i \partial q_j}\left(\chi_{ij}^{vv}\right)$$

$$= \frac{\partial^2}{\partial q_i \partial q_j}\left(\chi_{ij}^{uv}\right) = \frac{\partial^2}{\partial q_i \partial q_j}\left(\chi_{ij}^{vu}\right), \tag{11A}$$

where

$$q_i \equiv \ell n\ p_i, \quad q_j \equiv \ell n\ p_j,$$

and the other symbols are the same as in the text.

Since the χ_{ij} are functions of p_i and p_j only, and since they are required to approach zero as the pressure separation $p_i - p_j$ becomes large, then (9A), (10A), and (11A) are equivalent to

$$\chi_{ij}^{uv} = \chi_{ij}^{vu} = \chi_{ij}^{vv} = \chi_{ij}^{uu} \tag{12A}$$

$$\chi_{ij}^{ut} = \chi_{ij}^{vt} = \frac{\partial}{\partial q_j}\left(\chi_{ij}^{uu}\right) \tag{13A}$$

$$\chi_{ij}^{tu} = \chi_{ij}^{tv} = \frac{\partial}{\partial q_i}\left(\chi_{ij}^{uu}\right) \tag{14A}$$

$$\chi_{ij}^{tt} = \frac{\partial^2}{\partial q_i \partial q_j}\left(\chi_{ij}^{uu}\right) \tag{15A}$$

Thus, by means of the thermal wind relation and the factoring assumption, all of the quasi-horizontal functions can be expressed in terms of ψ_{ij}^{tt} and all of the vertical functions in terms of χ_{ij}^{uu}.

In order to express these functional relations in terms of correlations, define

$$\mu_{ij}^{tt} \equiv \psi_{ij}^{tt} / \left(\psi_{ii}^{tt}\ \psi_{jj}^{tt}\right)^{\frac{1}{2}}, \tag{16A}$$

$$\mu_{ij}^{ut} \equiv \psi_{ij}^{ut} / \left(\psi_{ii}^{uu}\ \psi_{jj}^{tt}\right)^{\frac{1}{2}}, \tag{17A}$$

etc., for the quasi-horizontal functions, and

$$\nu_{ij}^{tt} = \chi_{ij}^{tt} / \left(\chi_{ii}^{tt}\ \chi_{jj}^{tt}\right)^{\frac{1}{2}}, \tag{18A}$$

$$\nu_{ij}^{ut} = \chi_{ij}^{ut} / \left(\chi_{ii}^{uu}\ \chi_{jj}^{tt}\right)^{\frac{1}{2}}, \tag{19A}$$

etc., for the vertical functions. In the above, an "ii" subscript indicates the limit value of a function when j→i, and a "jj" subscript indicates the value when i→j. Clearly, the total correlations are given by

$$\frac{\overline{t_i t_j}}{\left(\overline{t_i^2}\,\overline{t_j^2}\right)^{\frac{1}{2}}} \equiv \rho_{ij}^{tt} = \mu_{ij}^{tt}\ \nu_{ij}^{tt}\ , \tag{20A}$$

$$\frac{\overline{u_i t_j}}{\left(\overline{u_i^2}\,\overline{t_j^2}\right)^{\frac{1}{2}}} \equiv \rho_{ij}^{ut} = \mu_{ij}^{ut}\ \nu_{ij}^{ut}\ , \tag{21A}$$

etc.

The analysis scheme currently assumes that

$$\psi_{ij}^{tt} = C\ \exp\left[-\ k_h \left(\Delta S_{ij}\right)^2\right]\ , \tag{22A}$$

where C is a constant with the dimensions deg^2, and that

$$\chi_{ij}^{uu} = \frac{1}{1+k_p\, \ell n^2 (P_i/P_j)} = \frac{1}{1+k_p (q_i - q_j)^2}\ . \tag{23A}$$

If (22A) is substituted in (1A) through (7A) and the resulting expressions normalized as indicated by (16A) and (17A), the results are

$$\mu_{ij}^{tt} = \exp\left[-\ k_h (\Delta S_{ij})^2\right] \tag{24A}$$

$$\mu_{ij}^{ut} = -\ \frac{(2k_h)^{\frac{1}{2}}}{\overline{m}} (y_i - y_j) \mu_{ij}^{tt} \tag{25A}$$

$$\mu_{ij}^{tu} = \frac{(2k_h)^{\frac{1}{2}}}{\overline{m}}(y_i - y_j)\mu_{ij}^{tt} \tag{26A}$$

$$\mu_{ij}^{vt} = \frac{(2k_h)^{\frac{1}{2}}}{\overline{m}}(x_i - x_j)\mu_{ij}^{tt} \tag{27A}$$

$$\mu_{ij}^{tv} = -\frac{(2k_h)^{\frac{1}{2}}}{\overline{m}}(x_i - x_j)\mu_{ij}^{tt} \tag{28A}$$

$$\mu_{ij}^{uu} = [1 - \frac{2k_h}{\overline{m}^2}(y_i - y_j)^2]\mu_{ij}^{tt} \tag{29A}$$

$$\mu_{ij}^{vv} = [1 - \frac{2k_h}{\overline{m}^2}(x_i - x_j)^2]\mu_{ij}^{tt} \tag{30A}$$

$$\mu_{ij}^{uv} = \mu_{ij}^{vu} = \frac{2k_h}{\overline{m}^2}(x_i - x_j)(y_i - y_j)\mu_{ij}^{tt} \tag{31A}$$

Similarly, substitution of (23A) in (12A) through (15A) and normalizing as in (18A) and (19A) gives

$$\nu_{ij}^{vv} = \nu_{ij}^{uv} = \nu_{ij}^{vu} = \nu_{ij}^{uu} = \frac{1}{1 + k_p \ell n^2(P_i/P_j)} \tag{32A}$$

$$\nu_{ij}^{ut} = \nu_{ij}^{vt} = (2k_p)^{\frac{1}{2}} \ell n(P_i/P_j)(\nu_{ij}^{uu})^2 \tag{33A}$$

$$\nu_{ij}^{tu} = \nu_{ij}^{tv} = -(2k_p)^{\frac{1}{2}} \ell n(P_i/P_j)(\nu_{ij}^{uu})^2 \tag{34A}$$

$$\nu_{ij}^{tt} = [1 - 4k_p \ell n^2(P_i/P_j)\nu_{ij}^{uu}](\nu_{ij}^{uu})^2 \tag{35A}$$

Expressions (24A) through (35A) give the correlations currently used in the analysis scheme and depicted in Figs. 1 and 2.

When functional forms for ψ_{ij}^{tt} and χ_{ij}^{uu} are assumed as in (22A) and (23A), functional representations of the mean square quantities $\overline{t_i^2}$, $\overline{u_i^2}$, and $\overline{v_i^2}$ are also implicitly assumed. Using (5A), (6A), (15A), and the equality of χ_{ij}^{uu} and χ_{ij}^{vv} in (12A),

$$\overline{t_i^2} = \psi_{ii}^{tt}\,\chi_{ii}^{tt} = \psi_{ii}^{tt}\,\frac{\partial^2}{\partial q_i \partial q_j}\left(\chi_{ij}^{uu}\right)\Big|_{j=i}\,, \tag{36A}$$

$$\overline{u_i^2} = \psi_{ii}^{uu}\,\chi_{ii}^{uu} = \frac{R^2 G_i^2}{f_i^2}\,\frac{\partial^2}{\partial y_i \partial y_j}\left(\psi_{ij}^{tt}\right)\Big|_{j=i}\,\chi_{ii}^{uu}\,, \tag{37A}$$

$$\overline{v_i^2} = \psi_{ii}^{vv}\,\chi_{ii}^{vv} = \frac{R^2 G_i^2}{f_i^2}\,\frac{\partial^2}{\partial y_i \partial y_j}\left(\psi_{ij}^{tt}\right)\Big|_{j=i}\,\chi_{ii}^{uu}\,. \tag{38A}$$

For the choices (22A) and (23A) for ψ_{ij}^{tt} and χ_{ij}^{uu}, these expressions yield

$$\overline{t_i^2} = 2C\,k_p \tag{39A}$$

and

$$\overline{u_i^2} = \overline{v_i^2} = 2C\,k_h\,R^2 G_i^2/f_i^2\,, \tag{40A}$$

that is, $\overline{t_i^2}$ is assumed constant, and $\overline{u_i^2}$ and $\overline{v_i^2}$ are assumed equal and a function of latitude only.

Appendix B: Derivation of Correlation Functions for Use of Geopotential Height Data in Upper-Air Analysis

Part 1: Height-temperature relationships.

Equations (3.1) and (3.2) of the text assume that corrections made to the temperature and those made to the wind components are related by the thermal wind relation. If, additionally, the geopotential height and the wind components are geostrophically related, i.e.,

$$u = -\frac{Gg}{f}\frac{\partial z}{\partial y}, \tag{1B}$$

$$v = \frac{Gg}{f}\frac{\partial z}{\partial x}, \tag{2B}$$

where g is the acceleration due to gravity, and other symbols are the same as in the text, then, substituting (1B) and (2B) in (3.1) and (3.2),

$$\frac{\partial t}{\partial x} = -\frac{g}{R}\frac{\partial^2 z}{\partial q \partial x}, \tag{3B}$$

$$\frac{\partial t}{\partial y} = -\frac{g}{R}\frac{\partial^2 z}{\partial q \partial y}, \tag{4B}$$

where $q \equiv \ell n(p)$. If (3B) and (4B) are true, then the covariances between two points, i and j, of the variables z and t are related as follows:

$$\frac{\partial}{\partial x_i}\left(\overline{t_i z_j}\right) = -\frac{g}{R}\frac{\partial^2}{\partial q_i \partial x_i}\left(\overline{z_i z_j}\right) \tag{5B}$$

$$\frac{\partial}{\partial x_j}\left(\overline{z_i t_j}\right) = -\frac{g}{R}\frac{\partial^2}{\partial q_j \partial x_j}\left(\overline{z_i z_j}\right) \tag{6B}$$

$$\frac{\partial}{\partial y_i}\left(\overline{t_i z_j}\right) = -\frac{g}{R}\frac{\partial^2}{\partial q_i \partial y_i}\left(\overline{z_i z_j}\right) \tag{7B}$$

$$\frac{\partial}{\partial y_j}\left(\overline{z_i t_j}\right) = -\frac{g}{R}\frac{\partial^2}{\partial q_j \partial y_j}\left(\overline{z_i z_j}\right) \tag{8B}$$

$$\frac{\partial^2}{\partial x_i \partial x_j}\left(\overline{t_i t_j}\right) = \frac{g^2}{R^2}\frac{\partial^2}{\partial q_i \partial q_j}\frac{\partial^2}{\partial x_i \partial x_j}\left(\overline{z_i z_j}\right) \tag{9B}$$

$$\frac{\partial^2}{\partial y_i \partial y_j}\left(\overline{t_i t_j}\right) = \frac{g^2}{R^2}\frac{\partial^2}{\partial q_i \partial q_j}\frac{\partial^2}{\partial y_i \partial y_j}\left(\overline{z_i z_j}\right) \tag{10B}$$

Assume that

$$\overline{z_i z_j} = \psi_{ij}^{zz}(x_i, y_i; x_j, y_j)\chi_{ij}^{zz}(p_i, p_j), \tag{11B}$$

$$\overline{t_i z_j} = \psi_{ij}^{tz}(x_i, y_i; x_j, y_j)\chi_{ij}^{tz}(p_i, p_j), \tag{12B}$$

etc. Substituting these expressions in (5B) through (10B) yields

$$\frac{\partial}{\partial x_i}\left(\psi_{ij}^{tz}\right) = -\frac{g}{R}\frac{\partial}{\partial x_i}\left(\psi_{ij}^{zz}\right), \tag{13B}$$

$$\frac{\partial}{\partial x_j}\left(\psi_{ij}^{zt}\right) = -\frac{g}{R}\frac{\partial}{\partial x_j}\left(\psi_{ij}^{zz}\right), \tag{14B}$$

$$\frac{\partial^2}{\partial x_i \partial x_j}\left(\psi_{ij}^{tt}\right) = \frac{g^2}{R^2}\frac{\partial^2}{\partial x_i \partial x_j}\left(\psi_{ij}^{zz}\right), \tag{15B}$$

plus three similar equations in terms of derivatives with respect to y_i and y_j. Also

$$\chi_{ij}^{tz} = \frac{\partial}{\partial q_i}\left(\chi_{ij}^{zz}\right), \tag{16B}$$

$$\chi_{ij}^{zt} = \frac{\partial}{\partial q_j}\left(\chi_{ij}^{zz}\right), \tag{17B}$$

$$\chi_{ij}^{tt} = \frac{\partial^2}{\partial q_i \partial q_j}\left(\chi_{ij}^{zz}\right). \tag{18B}$$

From (13B) through (15B) and the similar equations in y_i, y_j,

$$\psi_{ij}^{tz} = -\frac{g}{R}\psi_{ij}^{zz} + \text{constant},$$

etc., and, since the functions are required to approach zero for large separations of points i and j,

$$\psi_{ij}^{tt} = -\frac{g}{R}\psi_{ij}^{tz} = -\frac{g}{R}\psi_{ij}^{zt} = \frac{g^2}{R^2}\psi_{ij}^{zz} \tag{19B}$$

As in Appendix A, define

$$\mu_{ij}^{zz} \equiv \psi_{ij}^{zz}/\left(\psi_{ii}^{zz}\psi_{jj}^{zz}\right)^{\frac{1}{2}}, \tag{20B}$$

$$\mu_{ij}^{tz} \equiv \psi_{ij}^{tz}/\left(\psi_{ii}^{tt}\psi_{jj}^{zz}\right)^{\frac{1}{2}}, \tag{21B}$$

etc., as quasi-horizontal correlations, and

$$\nu_{ij}^{zz} \equiv \chi_{ij}^{zz}/\left(\chi_{ii}^{zz}\chi_{jj}^{zz}\right)^{\frac{1}{2}}, \tag{22B}$$

$$\nu_{ij}^{tz} = \chi_{ij}^{tz}/\left(\chi_{ii}^{tt}\chi_{jj}^{zz}\right)^{\frac{1}{2}}, \tag{23B}$$

etc., as vertical correlations. Then

$$\rho_{ij}^{zz} = \mu_{ij}^{zz}\nu_{ij}^{zz}, \tag{24B}$$

$$\rho_{ij}^{tz} = \mu_{ij}^{tz}\nu_{ij}^{tz}, \tag{25B}$$

etc. To express these correlations in terms of correlations derived in Appendix A, note that, for any choice of ψ_{ij}^{zz}, (19B) gives

$$\psi_{ii}^{tt} = \frac{g^2}{R^2}\,\psi_{ii}^{zz} \tag{26B}$$

and similarly for ψ_{jj}^{tt}. Hence, normalization of (19B) using (20B), (21B), etc., and (26B) gives

$$\mu_{ij}^{zz} = -\,\mu_{ij}^{zt} = -\,\mu_{ij}^{tz} = \mu_{ij}^{tt} \tag{27B}$$

For the vertical correlations, compare (18B) with (15A) of Appendix A. Obviously,

$$\chi_{ii}^{zz} = \chi_{ii}^{uu}\,, \tag{28B}$$

except for a constant term which we require to be zero. It follows that

$$\nu^{zz} = \nu^{uu} \tag{29B}$$

$$\nu^{tz} = \nu^{tu} \tag{30B}$$

$$\nu^{zt} = \nu^{ut} \tag{31B}$$

Part 2: Height-wind relationships.

The geostrophic relation between height corrections and wind component corrections given by (1B) and (2B) leads to the following covariance relations:

$$\overline{u_i z_j} = -\frac{G_i g}{f_i}\frac{\partial}{\partial y_i}\left(\overline{z_i z_j}\right), \tag{32B}$$

$$\overline{z_i u_j} = -\frac{G_j g}{f_j}\frac{\partial}{\partial y_j}\left(\overline{z_i z_j}\right), \tag{33B}$$

$$\overline{v_i z_j} = \frac{G_i g}{f_i}\frac{\partial}{\partial x_i}\left(\overline{z_i z_j}\right), \tag{34B}$$

$$\overline{z_i v_j} = \frac{G_j g}{f_j}\frac{\partial}{\partial x_j}\left(\overline{z_i z_j}\right), \tag{35B}$$

$$\overline{u_i u_j} = \frac{G_i G_j g^2}{f_i f_j}\frac{\partial^2}{\partial y_i \partial y_j}\left(\overline{z_i z_j}\right), \tag{36B}$$

plus three more such relations analogous to (3.11) through (3.13) of the text. Separating (32B) through (36B) into equations in $(x_i, y_j; y_i, y_j)$ and (p_i, p_j) leads to

$$\psi_{ij}^{uz} = -\frac{G_i g}{f_i}\frac{\partial}{\partial y_i}\left(\psi_{ij}^{zz}\right) \tag{37B}$$

$$\psi_{ij}^{zu} = -\frac{G_j g}{f_j}\frac{\partial}{\partial y_j}\left(\psi_{ij}^{zz}\right) \tag{38B}$$

$$\psi_{ij}^{vz} = \frac{G_i g}{f_i}\frac{\partial}{\partial x_i}\left(\psi_{ij}^{zz}\right) \tag{39B}$$

$$\psi_{ij}^{zv} = \frac{G_j g}{f_j}\frac{\partial}{\partial x_j}\left(\psi_{ij}^{zz}\right) \tag{40B}$$

$$\psi_{ij}^{uu} = \frac{G_i G_j g^2}{f_i f_j}\frac{\partial^2}{\partial y_i \partial y_j}\left(\psi_{ij}^{zz}\right), \tag{41B}$$

Kistler, R. E., and R. D. McPherson, 1975: On the use of a local wind correction technique in four-dimensional data assimilation. Mon. Wea. Rev., 103, 431-444.

Kluge, J., 1970: Ausmitzung der Winddaten bei der numerischen analyse des geopotentials der AT der mittleren troposphäre mittels optimaler interpolation. Zeitzchrift für Meteorologie, 21, 286-292.

Krishnamurti, T. N., 1968: A diagnostic balance model for studies of weather systems at low and high latitudes, Rossby number less than one. Mon. Wea. Rev., 96, 197-207.

Kruger, H. B., 1969: General and special approaches to the problem of objective analysis of meteorological fields. Quart. J. Royal Meteor. Soc., 95, 21-39.

McPherson, R. D., K. H. Bergman, R. E. Kistler, G. E. Rasch, and D. S. Gordon, 1979: The NMC operational global data assimilation system. Mon. Wea. Rev., to be published in same issue of MWR as this paper.

Rutherford, I. D., 1973: Experiments on the updating of PE forecasts with real wind and geopotential data. Preprints, Third Conf. on Probability and Statistics in Atmos. Sciences, June 19-22, 1973, published by AMS, Boston, Mass., pp. 198-201.

_____ 1976: An operational three-dimensional multivariate statistical objective analysis scheme. GARP Report No. 11, Proc. of the JOC Study Group Conf. on Four-Dimensional Data Assimilation, Paris, 17-21 November 1975, 98-121.

Schlatter, T. W., 1975: Some experiments with a multivariate statistical objective analysis scheme. Mon. Wea. Rev., 103, 246-257.

and

$$\chi_{ij}^{zz} = \chi_{ij}^{uz} = \chi_{ij}^{zu} = \chi_{ij}^{vz} = \chi_{ij}^{zv} = \chi_{ij}^{uu} \ . \tag{42B}$$

Using (19B) to replace ψ_{ij}^{zz} with ψ_{ij}^{tt} in (37B) through (40B) results in

$$\psi_{ij}^{uz} = -\frac{G_i R^2}{g f_i} \frac{\partial}{\partial y_i} \left(\psi_{ij}^{tt}\right) \tag{43B}$$

and similar relations for ψ_{ij}^{zu}, ψ_{ij}^{vz}, and ψ_{ij}^{zv}. Comparison of (43B) with (1A) of Appendix A shows that

$$\psi_{ij}^{uz} = -\frac{R}{g} \psi_{ij}^{ut}, \tag{44B}$$

and similarly for ψ_{ij}^{zu}, ψ_{ij}^{vz}, and ψ_{ij}^{zv}. Defining μ-correlations as previously, normalizing (44B), etc., and using (26B) then gives

$$\mu_{ij}^{uz} = -\mu_{ij}^{ut} \tag{45B}$$

$$\mu_{ij}^{zu} = -\mu_{ij}^{tu} \tag{46B}$$

$$\mu_{ij}^{vz} = -\mu_{ij}^{vt} \tag{47B}$$

$$\mu_{ij}^{zv} = -\mu_{ij}^{tv}. \tag{48B}$$

From (42B) it immediately follows that

$$\nu_{ij}^{zz} = \nu_{ij}^{uz} = \nu_{ij}^{zu} = \nu_{ij}^{vz} = \nu_{ij}^{zv} = \nu_{ij}^{uu} \ . \tag{49B}$$

Thus, all of the new correlations involving a geopotential height correction are shown by (27B), (29B) through (31B), and (45B) through (49B) to be expressible in terms of correlations already derived in Appendix A for the (t,u,v) upper-air analysis.

REFERENCES

Beckman, F. S., 1960: The solution of linear equations by the conjugate gradient method. Mathematical Methods for Digital Computers, Vol. 1, A. Ralston and H. S. Wilf, Eds., Wiley, 62-72.

Belousov, S. L., L. S. Gandin, and S. A. Mashkovich, 1972: Computer Processing of Meteorological Data. (Translated by A. Nurlik) Meteorological Translation No. 18, Canada--Department of the Environment, Atmospheric Environment Service, Downsview, Ontario, Canada.

Bergman, K. H., 1976: Multivariate objective analysis of temperature and wind fields using the thermal wind relationship. Preprints, Sixth Conf. on Weather Forecasting and Analysis, May 10-13, 1976, Albany, N.Y. (AMS), 187-190.

_____ and W. D. Bonner, 1976: Analysis error as a function of observation density for satellite temperature soundings with spatially correlated errors. Mon. Wea. Rev., 104, 1308-1316.

_____ and D. S. Gordon, 1977: Spatial correlation of forecast errors and climatological variances for optimum interpolation analysis. Preprints, Fifth Conf. on Probability and Statistics in Atmospheric Sciences, Nov. 15-18, 1977, Las Vegas, Nev. (AMS), 79-84.

_____, 1978: The role of observational errors in optimum interpolation analysis. Bull. Am. Meteorol. Soc., 59, 1604-1611.

Desmarais, A. J., M. S. Tracton, R. D. McPherson, and R. J. van Haaren, 1978: The NMC report on the data systems test (NASA Contract S-70353-AG), Ch. 4; NOAA, U.S. Department of Commerce, Washington, D.C. (Available from National Technical Information Service, Springfield, Va. 22161)

Dey, C. H., and A. Caporaso, 1979: Objective verifications of the NMC data assimilation cycle. Office Note 197, National Meteorological Center, NWS/NOAA, Washington, D.C. 20233.

Druyan, L. M., 1972: Objective analysis of sea-level winds and pressure derived from simulated observations of a satellite radar-radiometer and actual conventional data. J. Applied Met., 11, 413-428.

Eddy. A., 1973: The objective analysis of atmospheric structure. J. Meteor. Soc. Japan, 51, 450-457.

Gandin, L. S., 1963: Objective analysis of meteorological fields. Gidrometeorologicheskoe Isdatel'stvo (GIMIZ), Leningrad. (Israel Program for Scientific Translations, Jerusalem, 1965, 242 pp.)

_____, R. L. Kagan, and A. I. Polishchuk, 1972: Estimation of the information content of meteorological observing systems. Leningr. Gl. Geofiz. Obser. Tr., No. 286, 120-140.

_____ and R. L. Kagan, 1974: Construction of a system for objective analysis of heterogeneous data based on the method of optimum interpolation and optimum agreement. Meteorologiya i Gidrologiva, 1974, No. 5 (Moscow), 1-11. (Translated by Joint Publications Research Service.)

Hollett, S. R., 1975: Three-dimensional spatial correlations of PE forecast errors. M.S. Thesis, Dept. of Meteorology, McGill Univ., P.O. Box 6070, Montreal H3C 3G1, Canada.

Julian, P. R., and H. J. Thiebaux, 1975: On some properties of correlation functions used in optimum interpolation schemes. Mon. Wea. Rev., 103, 605-616.

Schlatter, T. W.., G. W. Branstator, and L. G. Thiel, 1976: Testing a global multivariate statistical objective analysis scheme with observed data. Mon. Wea. Rev., 104, 765-783.

_____ , _____, and _____ , 1977: Reply [to Comments on a global objective analysis, H. J. Thiebaux]. Mon. Wea. Rev., 105, 1465-1468.

_____ , and G. W. Branstator, 1978: Errors in Nimbus 6 temperature profiles and their spatial correlation. NCAR Ms. 78/0501-1. National Center for Atmospheric Research, Boulder, Col., 90307. (Submitted for publication in Mon. Wea. Rev.)

Seaman, R. S., 1977: Absolute and differential accuracy of analyses achievable with specified observational network characteristics. Mon. Wea. Rev., 105.

Stackpole, J. D., L. W. Vanderman, and F. G. Shuman, 1974: The NMC 8-layer global primitive equation model on a latitude-longitude grid. Modelling for FGGE, GARP Publication Series No. 14, 79-93.

Stuart, D. W., 1974: A comparison of quasi-geostrophic vertical motion using various analyses. Mon. Wea. Rev., 102, 363-374.

Thiebaux, H. J., 1975: Experiments with correlation representations for objective analysis. Mon. Wea. Rev., 103, 617-627.

_____ 1976: Anisotropic correlation functions for objective analysis. Mon. Wea. Rev., 104, 994-1002.

Williamson, D. L., 1973: The effect of forecast error accumulation on four-dimensional data assimilation. J. Atmos. Sci., 30, 537-543.

TABLE 1. Mean Forecast Error Standard Deviation As A Function Of Pressure

Pressure (mb)	σ_ε T (^{o}c)	U (m s $^{-1}$)	V (m s $^{-1}$)
1000	4.3	4.9	4.6
850	3.2	4.2	4.1
700	2.2	4.3	4.0
500	2.0	4.9	4.7
400	2.1	5.7	5.6
300	2.6	7.1	6.7
250	3.4	7.5	7.2
200	3.6	7.3	7.0
150	3.1	6.7	6.4
100	3.0	5.6	5.4
70	2.9	6.0	6.3
50	4.6	9.0	9.8

TABLE 2. Normalized Observational Errors, ε_i

Variable	RAOB	ACRFT	VTPR	SATWIND
T	0.5	0.5	1.0	~
U,V	0.4	0.4	~	0.5

TABLE 3. Comparison of experimental 500-mb analyses for 0000 GMT 13 December 1977.

Run	Description	Max. No. of obs.	In screening, cross-correlations multiplied by	Normalized Estimated Errors T	Normalized Estimated Errors U,V	RMS differences from observed data T(°C)	RMS differences from observed data $\|\vec{V}\|$ (m sec^{-1})
A	6 hr. prediction (background fields)	0	-	1.0	1.0	1.85	13.97
B	Multivar. (T,U,V)	10	1.0	.621	.623	1.25	8.65
C	Multivar. (T,U,V)	10	1.75	.616	.625	1.26	8.65
D	Univar. T, Bivar. (U,V)	10	1.75	.634	.626	1.25	8.65
E	Multivar. (T,U,V)	20	1.75	.587	.594	1.30	9.13
F	Univar. T, Bivar. (U,V)	20	1.75	.622	.602	1.27	9.14
G	Multivar. (T,U,V)	6	1.75	.654	.647	1.22	8.64
H	Multivar. (T,U,V)	8	1.75	.634	.635	1.24	8.71
I	(U,V) obs. for T Anal. T obs. for (U,V) Anal.	10	1.75	.897	.932	1.76	14.04
J	Multivar. (T,U,V) ob. errors halved	10	1.75	(.561)	(.582)	1.15	7.98
K	Multivar. (T,U,V) ob. errors doubled	10	1.75	(.736)	(.713)	1.38	9.73
L	Multivar. (T,U,V) .25 k_h	10	1.75	(.526)	(.469)	1.42	10.88
M	Multivar. (T,U,V) 4 k_h	10	1.75	(.759)	(.788)	1.13	8.70

LIST OF FIGURES

9. Analysis of 500-mb temperatures, 0000 GMT 9 February 1975. Observed 500-mb temperatures shown for comparison.

10. The 10 observations used by optimum interpolation routine in adjusting 500-mb U component of wind at $50^{o}N/40^{o}W$. Symbols same as Fig. 7.

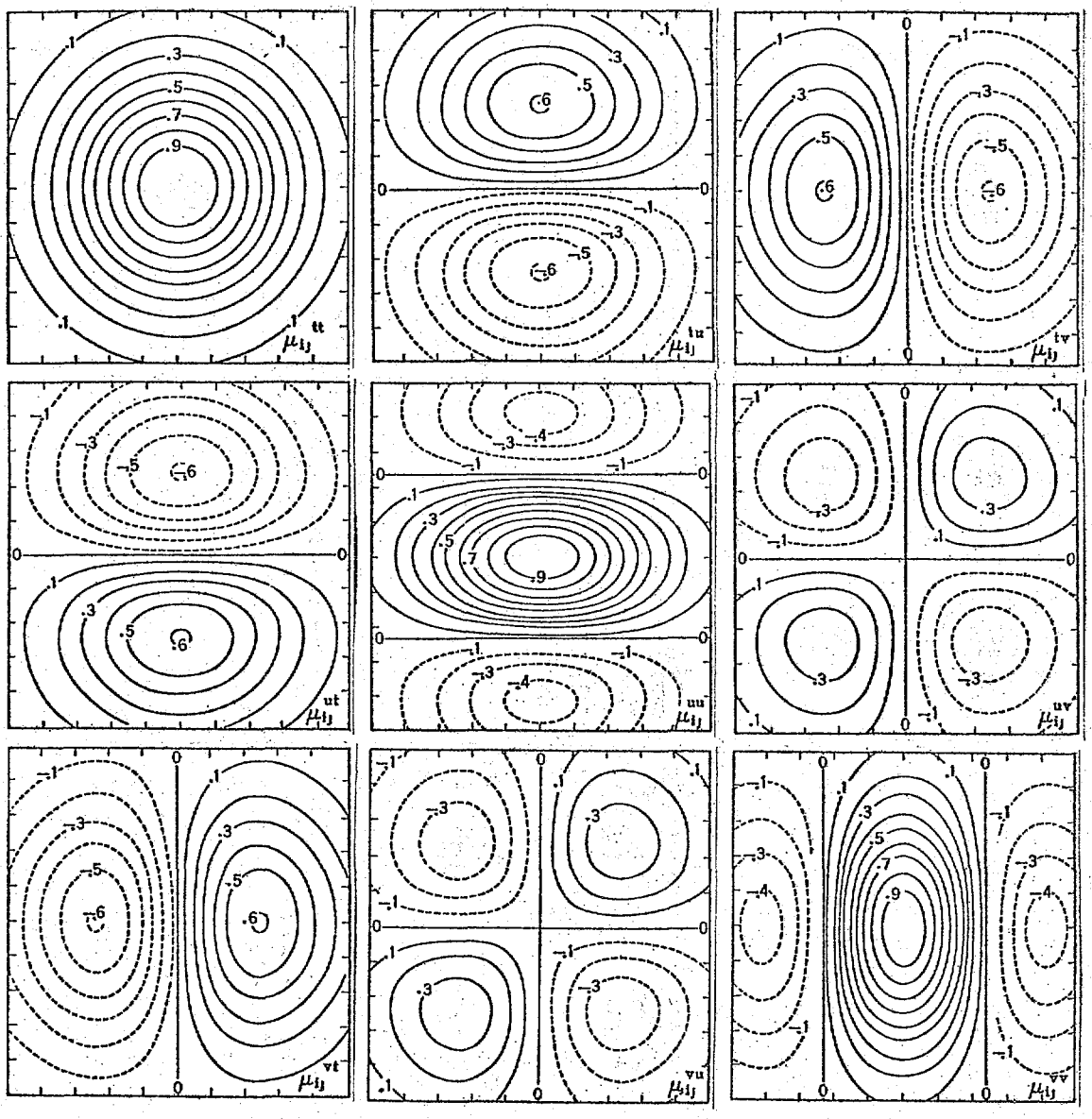
μ_{ij}^{tt}
μ_{ij}^{tu}
μ_{ij}^{tv}
μ_{ij}^{ut}
μ_{ij}^{uu}
μ_{ij}^{uv}
μ_{ij}^{vt}
μ_{ij}^{vu}
μ_{ij}^{vv}

Fig. 1

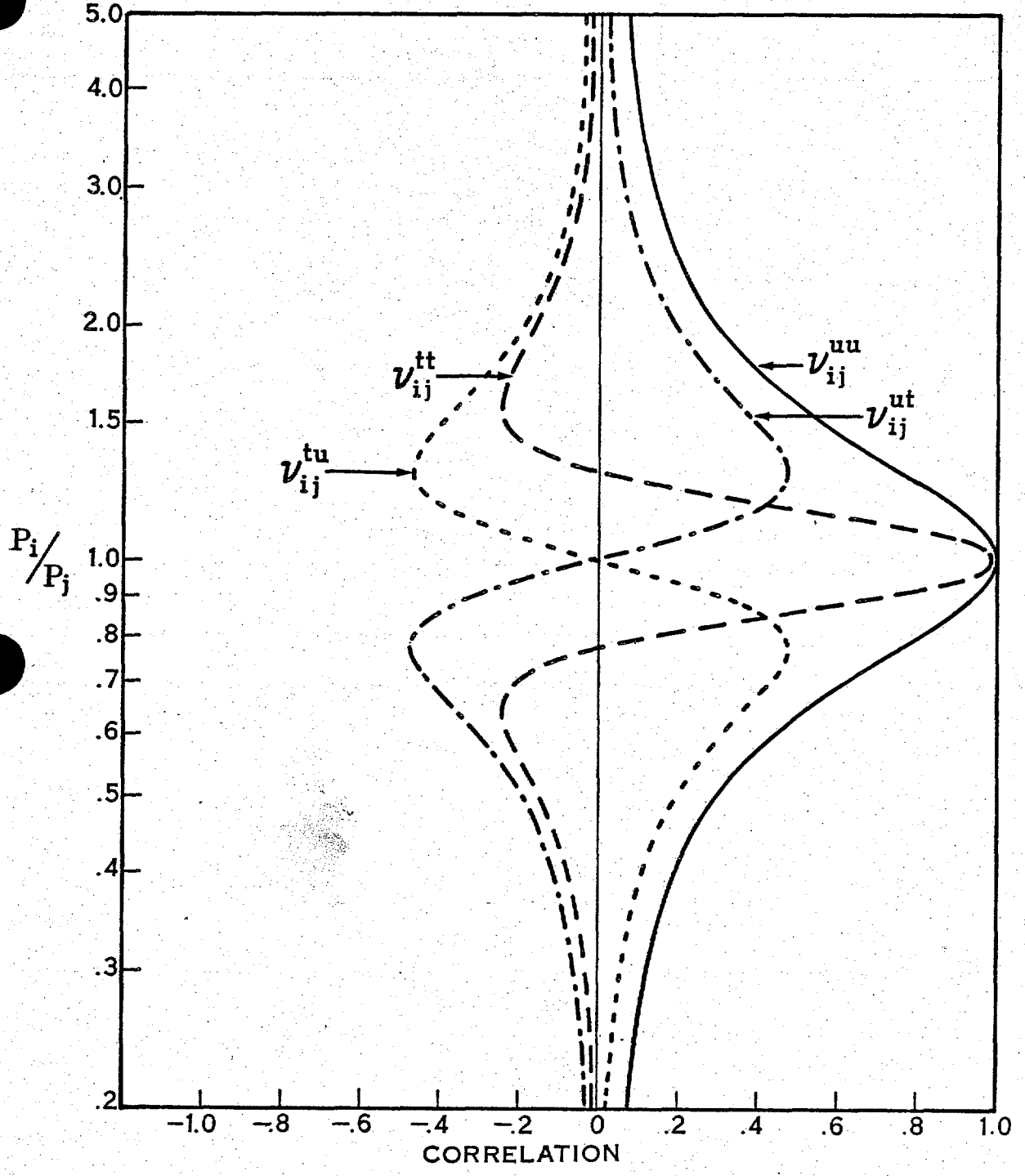
5.0
4.0
3.0
2.0
1.5
1.0
.9
.8
.7
.6
.5
.4
.3
.2
P_i/P_j
v_{ij}^{tt}
v_{ij}^{tu}
v_{ij}^{uu}
v_{ij}^{ut}
−1.0
−.8
−.6
−.4
−.2
0
.2
.4
.6
.8
1.0
CORRELATION

Fig. 2

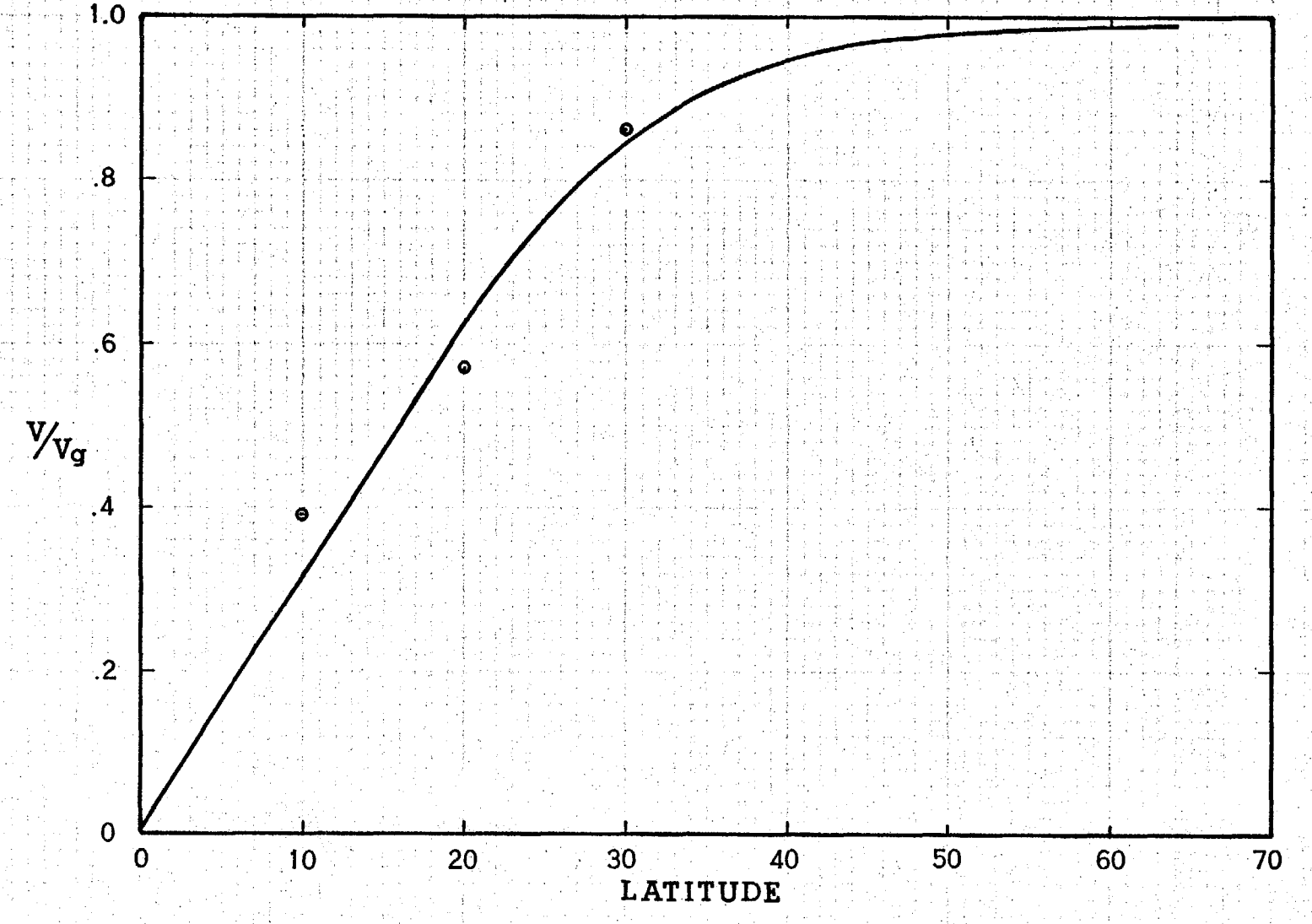

Fig. 3

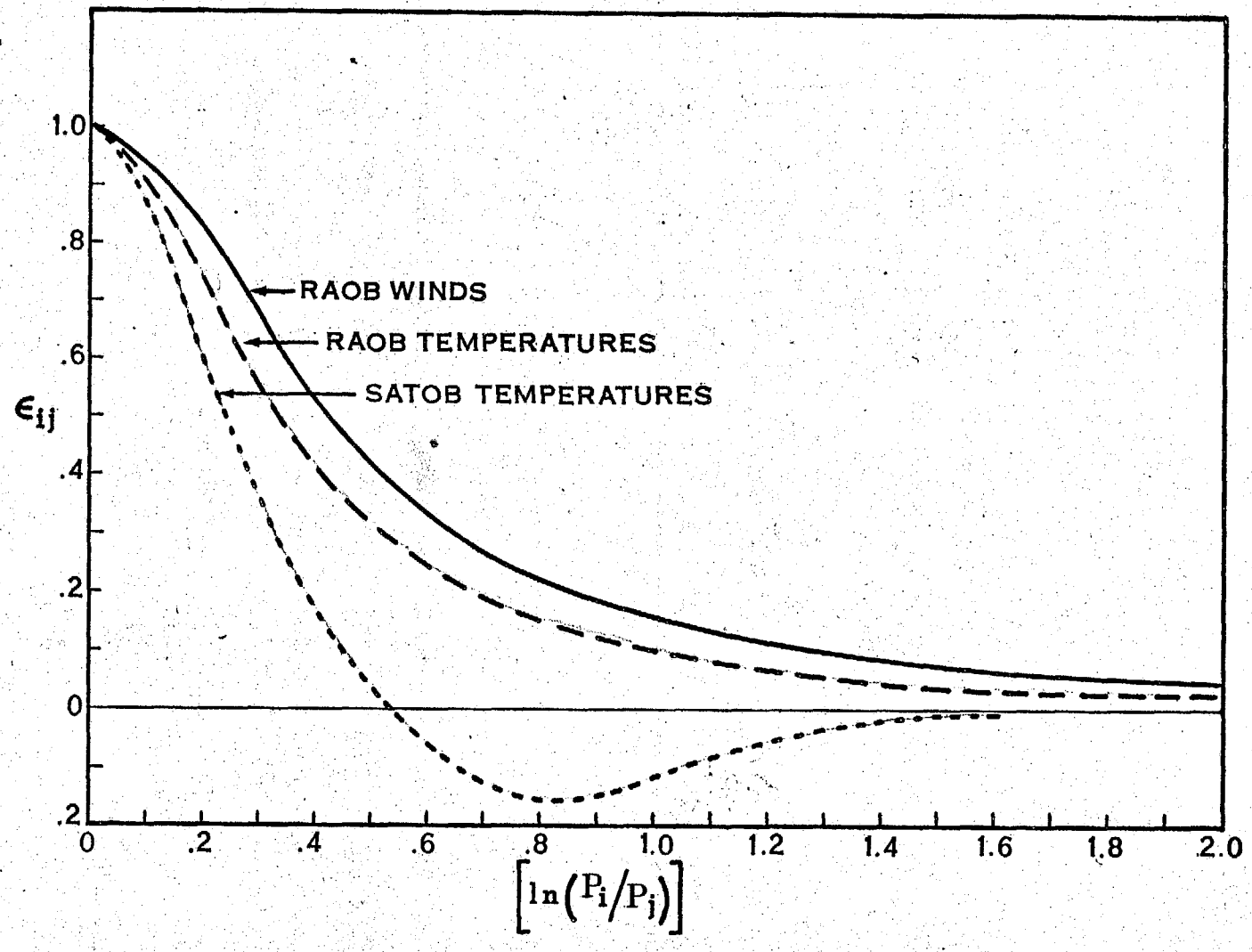
1.0
.8
.6
.4
.2
0
.2
ϵ_{ij}
RAOB WINDS
RAOB TEMPERATURES
SATOB TEMPERATURES
0
.2
.4
.6
.8
1.0
1.2
1.4
1.6
1.8
2.0
$\left[\ln\left(P_i/P_j\right)\right]$

Fig. 4

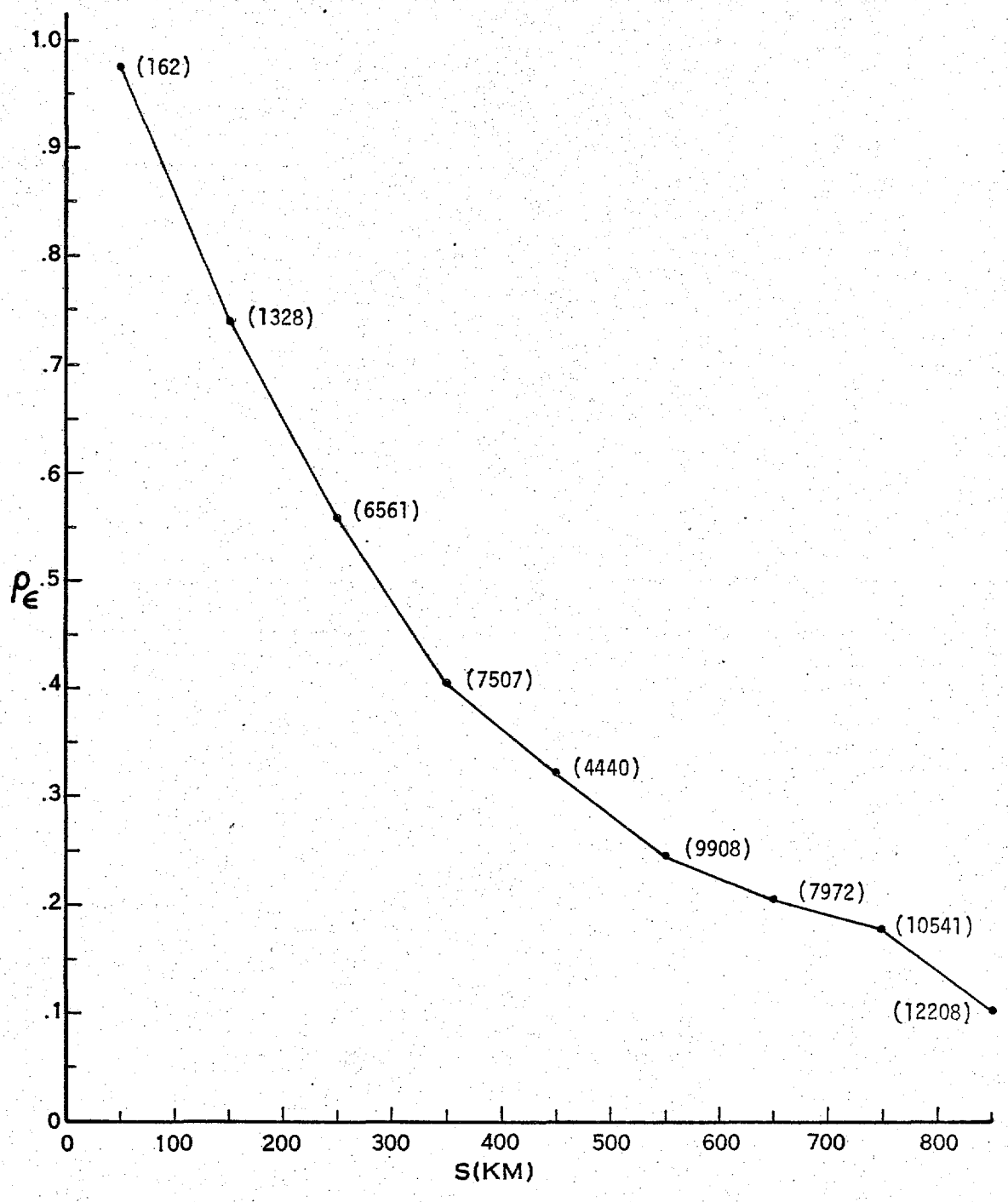
1.0
.9
.8
.7
.6
.5
.4
.3
.2
.1
0
ρ_ϵ
(162)
(1328)
(6561)
(7507)
(4440)
(9908)
(7972)
(10541)
(12208)
0
100
200
300
400
500
600
700
800
S(KM)

Fig. 5

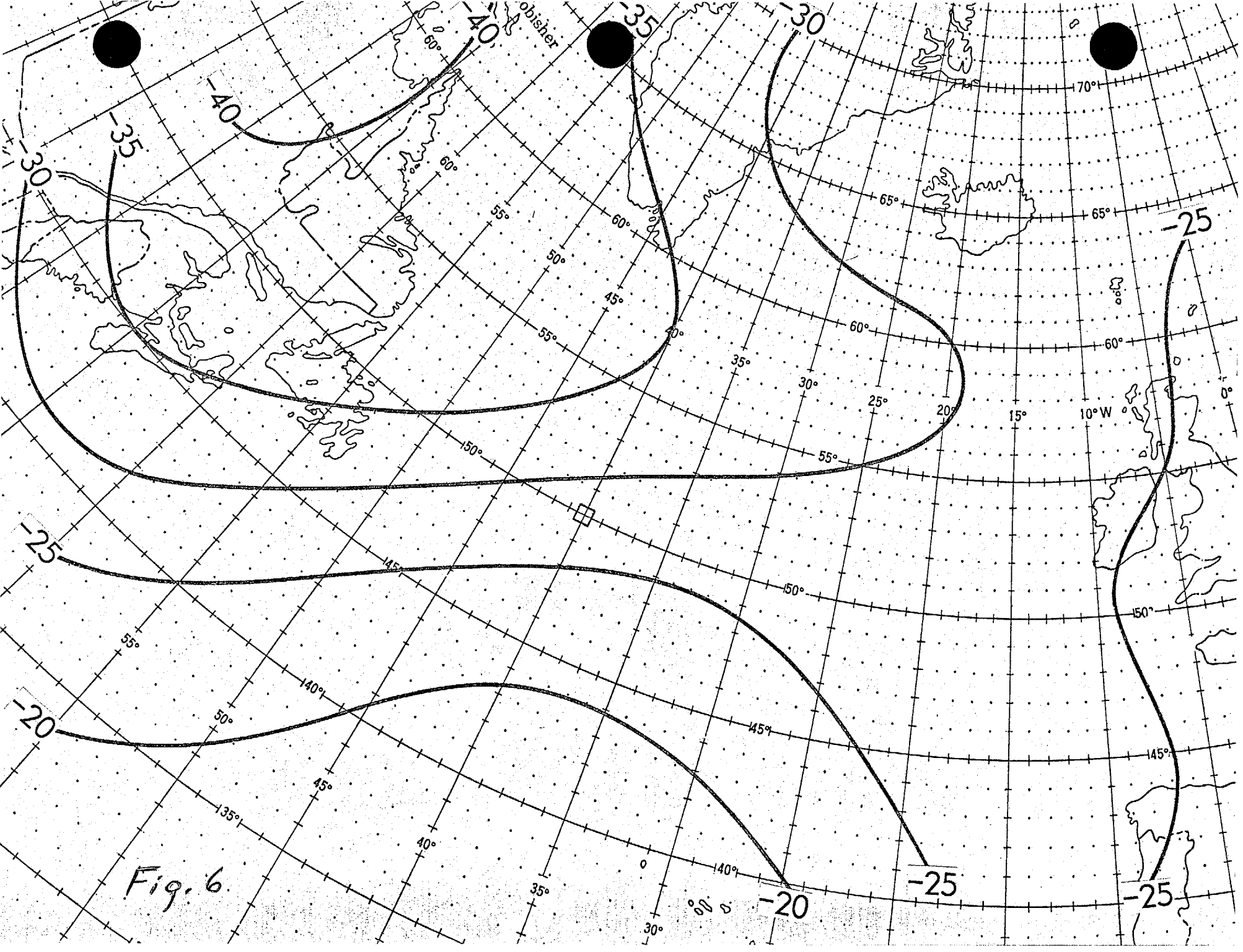
-40
-35
-30
-25
-20
Frobisher
70°
65°
60°
55°
50°
45°
40°
35°
30°
25°
20°
15°
10°W
0°
150°
145°
140°
135°

Fig. 6

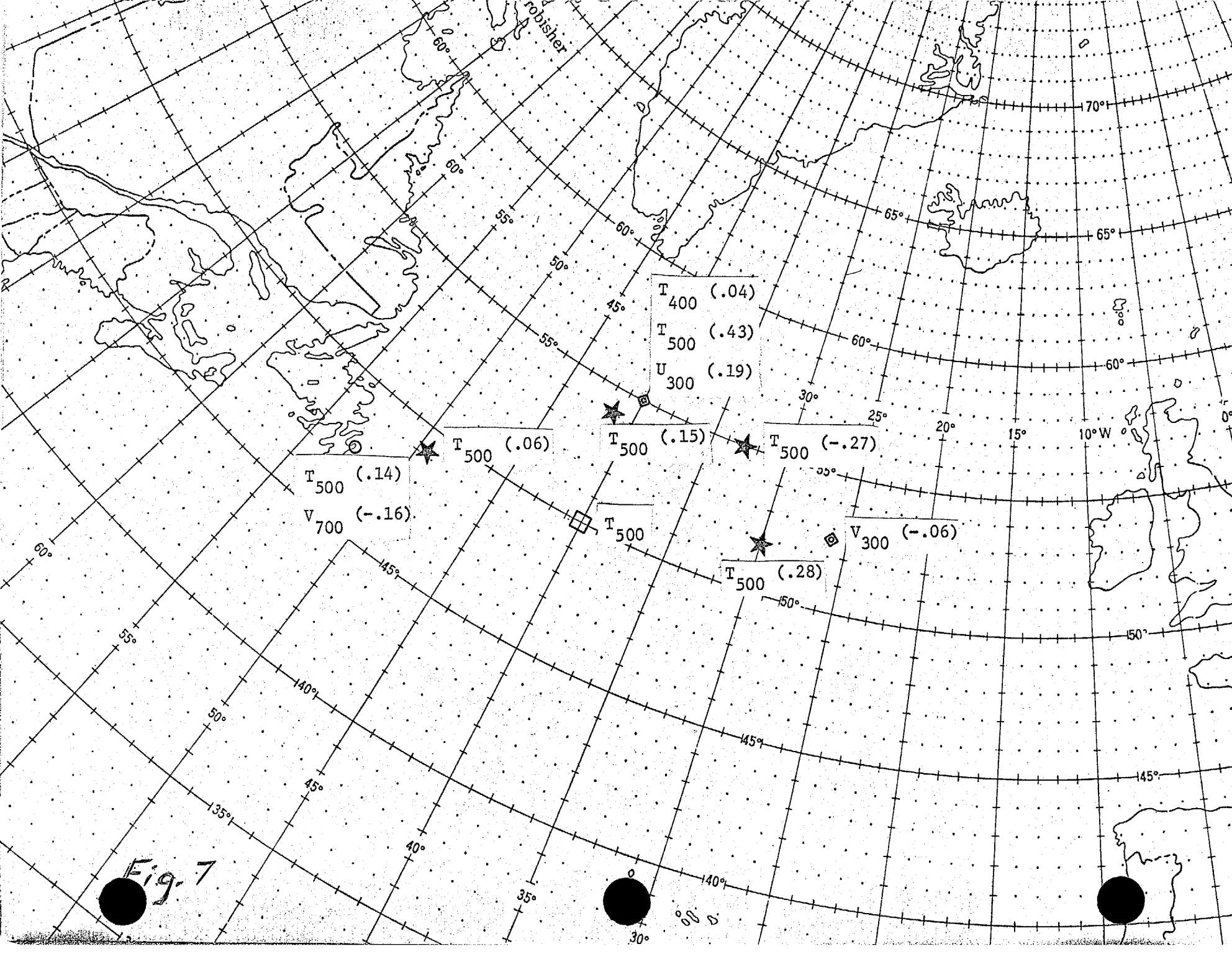
Frobisher
T_{400} (.04)
T_{500} (.43)
U_{300} (.19)
T_{500} (.06)
T_{500} (.15)
T_{500} (-.27)
T_{500} (.14)
V_{700} (-.16)
T_{500}
V_{300} (-.06)
T_{500} (.28)

Fig. 7

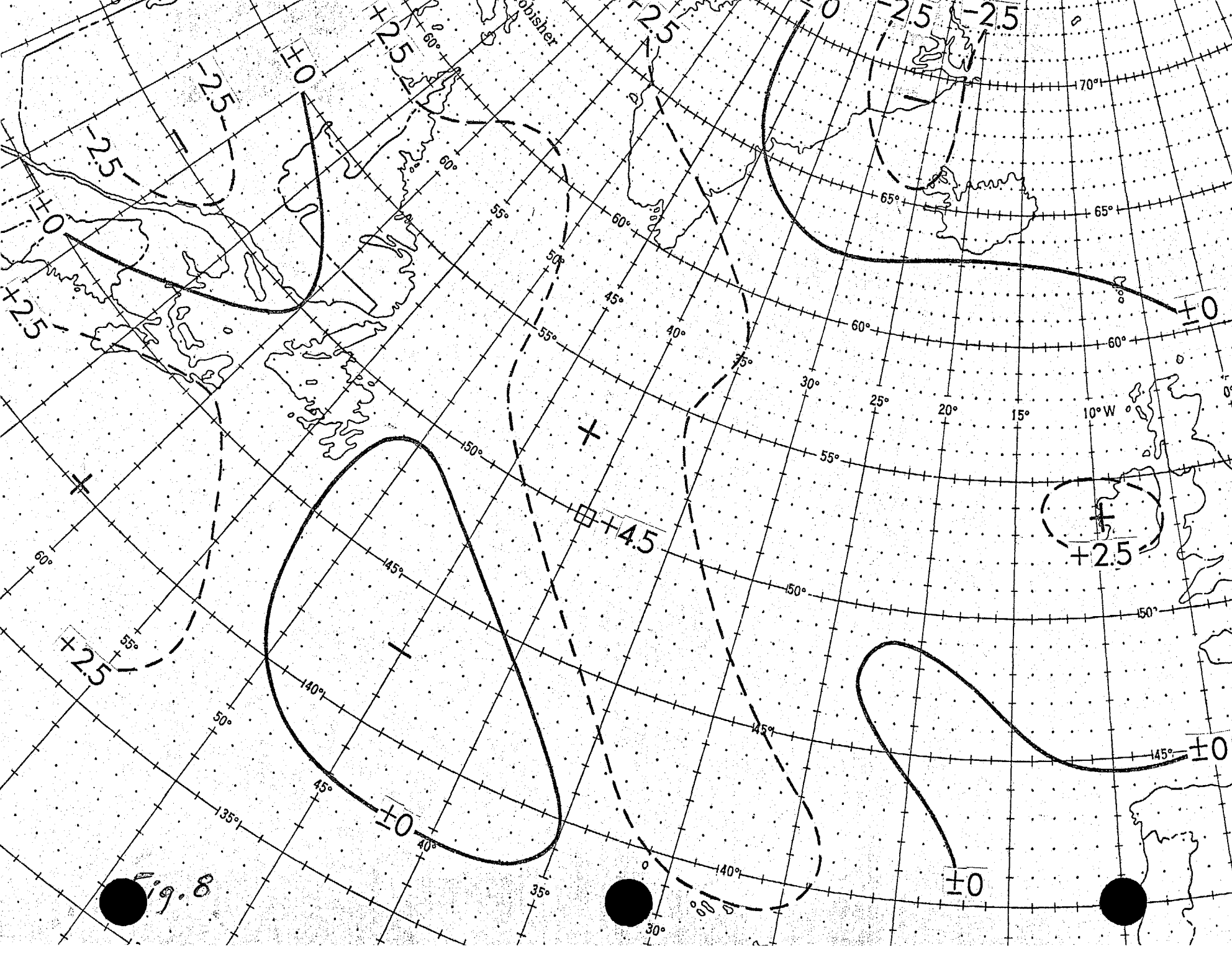
Frobisher
+0
-2.5
-2.5
+2.5
+0
+2.5
-2.5
-2.5
-2.5
+0
+0
+2.5
+2.5
+4.5
+2.5
+0
+0
+0
70°
65°
65°
60°
60°
55°
50°
45°
40°
35°
30°
30°
25°
20°
15°
10°W
0°
150°
145°
140°
135°

Fig. 8

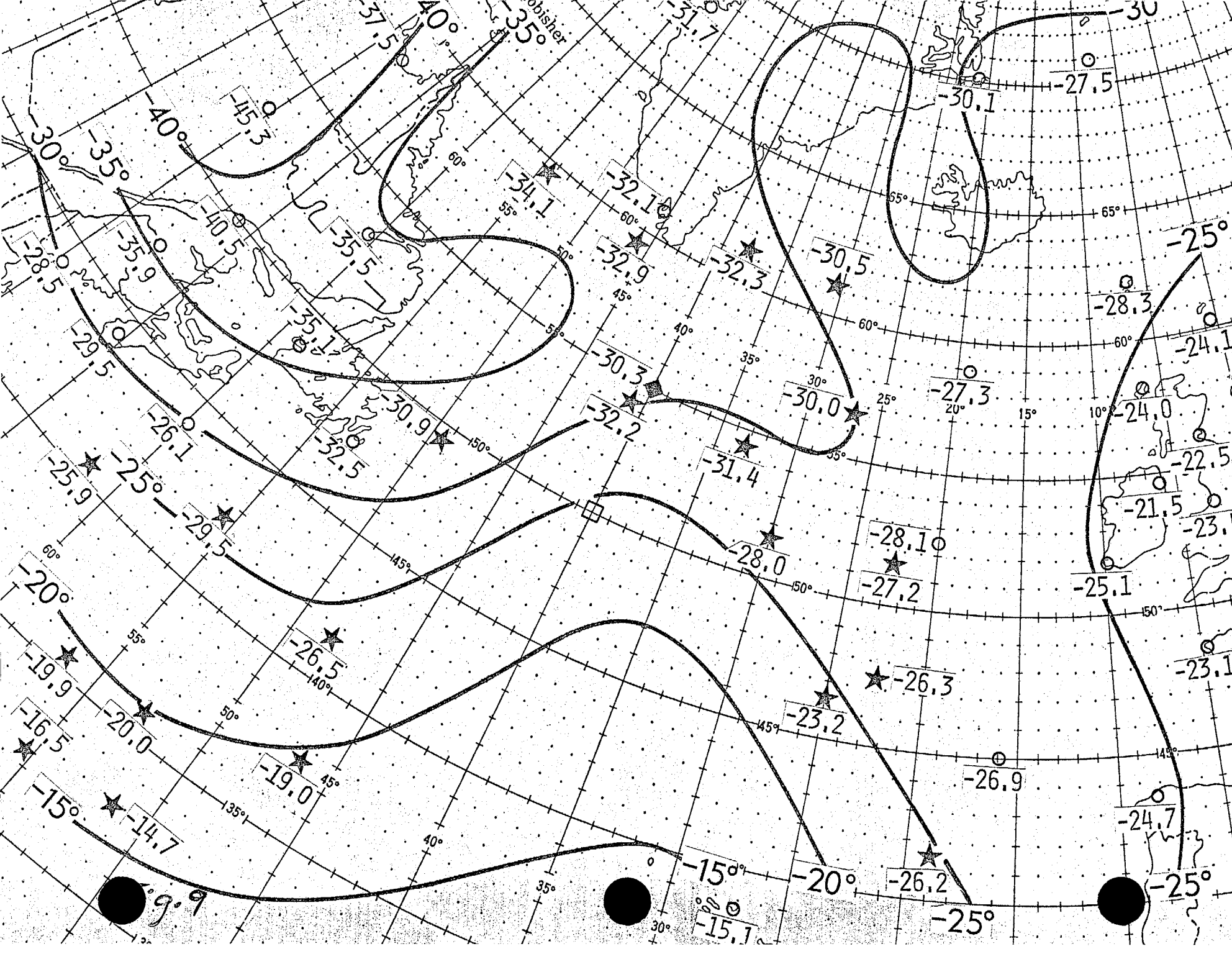
-30°
-35°
-40°
-37.5
-45.3
-34.1
-32.1
-31.7
-30
-27.5
-30.1
-35.5
-40.5
-35.9
-28.5
-29.5
-26.1
-35.1
-32.9
-32.3
-30.5
-28.3
-24.1
-25°
-30.3
-32.2
-30.9
-32.5
-31.4
-30.0
-27.3
-24.0
-22.5
-21.5
-25.9
-29.5
-28.0
-28.1
-27.2
-25.1
-23.1
-20°
-19.9
-20.0
-26.5
-26.3
-23.2
-16.5
-19.0
-26.9
-24.7
-15°
-14.7
-15°
-20°
-26.2
-25°
-25°
-15.1

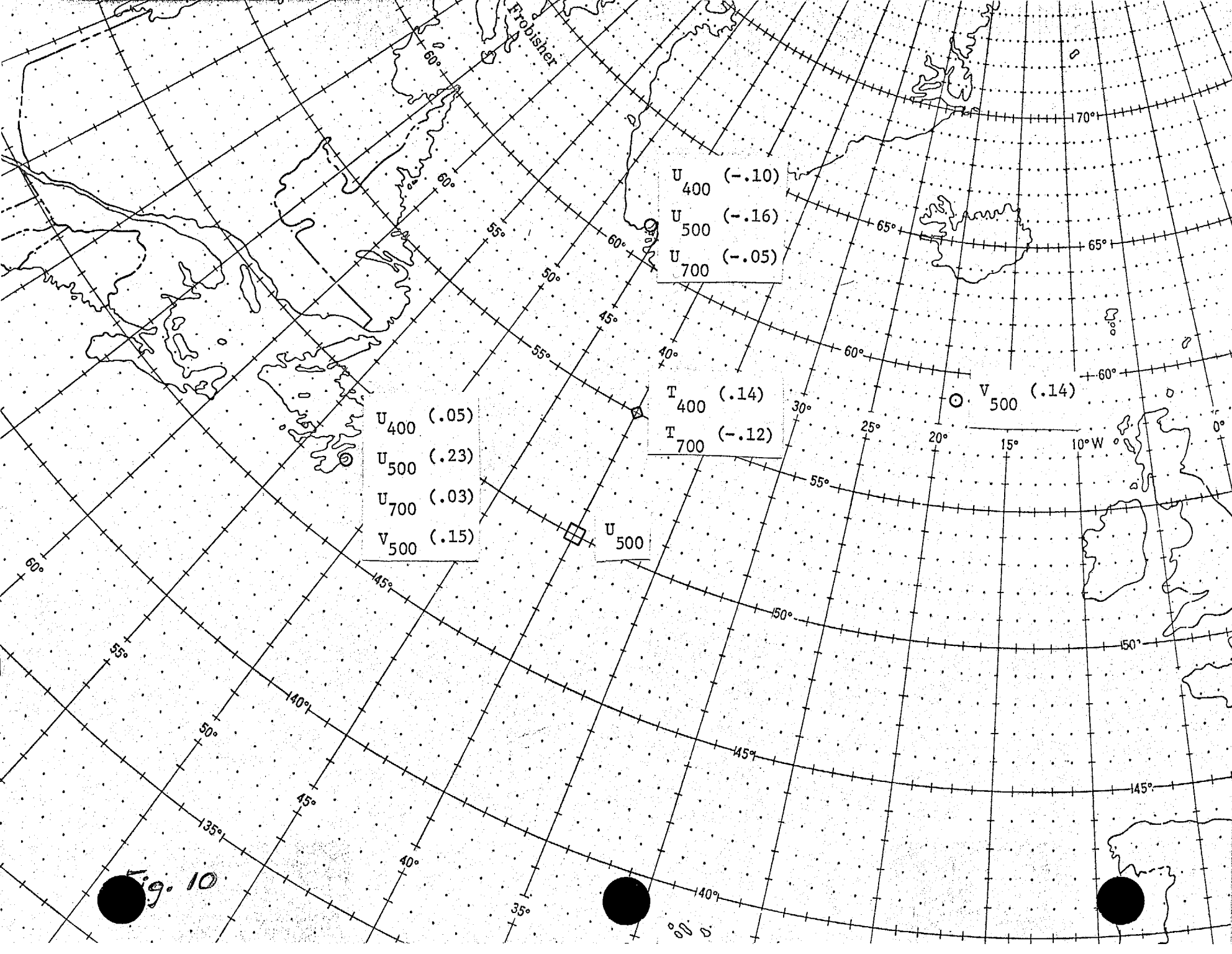
Frobisher
U_{400} (-.10)
U_{500} (-.16)
U_{700} (-.05)
T_{400} (.14)
T_{700} (-.12)
V_{500} (.14)
U_{400} (.05)
U_{500} (.23)
U_{700} (.03)
V_{500} (.15)
U_{500}
60°
55°
50°
45°
40°
35°
30°
25°
20°
15°
10°W
0°
65°
70°
135°
140°
145°
150°

Fig. 10